Institute of Water and Energy Sciences (Including Climate Change)

MODELLING RUNOFF, SOIL EROSION AND SEDIMENT YIELD IN SOSIANI CATCHMENT IN KENYA USING ARCSWAT

Johnstone Mainya

Date: 05/09/2017

*Master in **Water, Engineering track***

President: Dr. Tesfay Araya Weldeslassie

Supervisor: Prof. Benedict Mwavu Mutua

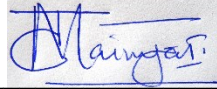**External Examiner: Dr. Mihret Dananto Ulsido**

Internal Examiner: Dr. Chewki Ziani Cherif

Academic Year: 2016-2017

DECLARATION AND RECOMMENDATION

DECLARATION

I declare that this thesis is my original work, and that it has not been wholly or in part presented for award of any degree in any University known to me.

Signature: _____   Date: _____7/08/2017_____

Name: **Johnstone Mainya**

RECOMMENDATION

This thesis is the candidate's original work and has been prepared with our guidance and assistance. It is presented for examination with our approval as official University Supervisors.
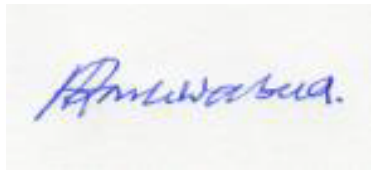
Signature: _____ Date: _____ **7/08/2017**____

Name: **Prof. Dr.-Ing. Benedict M. Mutua**

Department of Agricultural Engineering

Egerton University

Signature: _____Date: ___**7/08/2017**__

Name: **Dr. Raphael M. Wambua**

Department of Agricultural Engineering

Egerton University

Dedication

To my son, Dylan:

We all find something or someone to live for. And I found you.

Acknowledgement

Abstract

Sosiani catchment hosts Eldoret Town, a major agricultural, education and medical center in the Rift valley region of Kenya. Recent research has established that the quality of water in Sosiani River is rapidly deteriorating because of catchment erosion and wastes from industries. However, even though there have been efforts to control the pollution, non-point sources of pollution have not been characterized. The aim of this study was to simulate effect of rainfall magnitude on soil erosion, runoff and sediment yield in Sosiani catchment using ArcSWAT. The soil dataset used was obtained from Digital World Soil Map, weather datasets were obtained from Climate Forecast System Reanalysis (CFSR), DEM dataset was obtained from Open Topography, landuse/land cover dataset was obtained from USGS and river flow dataset was obtained from Water Resources Authority Kenya. The period of study was 1984-2012. Flow Calibration period was 1986-1990 while the validation period was 2008-2012. Sediment and soil erosion were not calibrated for lack of observed data. Flow calibration and validation results returned an R^2 value of 0.90 and 0.60 and NS value of -19.92 and -14.90. The study observed that increase in rainfall magnitude increased runoff, soil erosion and sediment yield except under conditions of increasing vegetative land cover. The study concludes that the model did not simulate the catchment correctly because it over-simulated both low and high flows. It recommends that datasets for the catchment (observed rainfall and river flows) need to be thoroughly checked for integrity before attempting to use them for hydrologic modelling. It further notes that agricultural land is the main contributor of sediment into river Sosiani and therefore remedial measures such as agroforestry and cover cropping would be appropriate immediate actions to control soil erosion.

Table of Contents

CHAPTER ONE

INTRODUCTION

Background Information

Modeling the effect of rainfall on runoff, soil erosion and sediment yield has been conducted by various studies in the world. For instance, Langbein and Schumm, (1958) suggested that sediment concentration in runoff increases with decrease in annual rainfall, while (Abbaspour, 2015a; Nearing *et al.,* 2005) observed that erosion and runoff increase with increase in rainfall magnitude and intensity. Morgan (2005) and Fang *et al.*(2012) noted that rainfall regimes with the most erosive effect include (i) those of events with high amounts, long duration and infrequent occurrence and (ii) those of events with medium amounts and medium duration. Cuomo, Della Sala, and Novità (2015) demonstrated that peak discharge of runoff and sediment increases with increase in rainfall intensity.

The effect of rainfall, coupled with land use changes can influence runoff, soil erosion and sediment yield (Kosmas *et al.,* 1997). For instance, soil erosion can be accelerated by decrease in land cover (Nearing *et al.,* 2005) and improper land use and management practices (Mutua, Klik, and Loiskandl, 2006). The natural relationship between rainfall, runoff, soil erosion, sediment yield and management practices on land is complex and is usually simplified and represented by use of models. Modelling provides appropriate Tools to evaluate the impact of management practices on runoff, soil erosion and sediment yield so as to plan for prime use of land within a catchment (Mutua *et al.,* 2006).

Soil is one of the most fundamental natural resources available to humans (Pimentel, 1993; Blanco-Canqui and Lal, 2010). Soil facilitates regulation of nutrient and water cycles. It helps to degrade complex materials and it exchanges gases with the atmosphere. It is also a suitable habitat for biodiversity (Waswa, 2012). According to FAO (2016), soil provides support and physical stability to plants, it is a source of construction materials, it has a spiritual value, it acts as a store of archaeological information and it is a ground for burial and heritage sites. These services that soil provides are essential to mitigate climate change, achieve food and water security and enhance quality of the environment.

Soil erosion is a continuous process by which soil particles are detached, and transported and deposited away mainly by the action of water, wind and humans. There are two major types of soil erosion; geologic and accelerated soil erosion. Geologic soil erosion, also called normal or natural erosion, takes place when the soil cover is unbroken and natural environmental elements are undisturbed. The rate is usually slow that the movement of the soil is hardly noticeable. The slow rate permits a state of equilibrium between the rate of soil removal and the rate of soil formation (Feng, 1995). On the other hand, accelerated soil erosion, also called anthropogenic soil erosion, takes place when the soil cover and stability of topsoil are broken and natural environmental elements are disturbed mainly by human-induced activities (Feng, 1995).

Anthropogenic soil erosion leads to loss of the quality of the soil. The loss limits the ability of soil to provide essential services. For example, it leads to extensive release of sediment and nutrients into streams, rivers, lakes and other water bodies. The sediment and nutrients deposited into water bodies negatively affect the quality of water (Feng, 1995; FAO, 2015). In economic sense, there is a high cost to soil erosion (Blanco-Canqui and Lal, 2010). Some of the costs include replenishment of lost soil nutrients, failure of water equipment, death of aquatic communities, desilting of reservoirs.

Growing demand for agricultural products provides incentive for conversion of forests and grasslands into agricultural lands. Such a conversion exposes soil to soil erosion at a rate that the soil loses the ability for self-sustenance (WWF, 2016). Water ecosystems that drain the agricultural lands often receive high amounts of eroded material such as sediment, pesticides, fertilizers and heavy metals. The material increase turbidity, destroy in-stream habitats and negatively impact on functions and services of the ecosystem (Wantzen and Mol, 2013). To control soil erosion, the first step is to monitor the location and extent of soil erosion. The second step is to develop data-based integrated catchment-level policy, legal, communication and technical strategy to control erosion. The third step is to implement soil erosion control and soil conservation techniques, starting with agricultural areas (Wantzen and Mol, 2013).

Soil erosion control and soil conservation methods are developed to reduce the impact of rain on the soil erosion, to strengthen the resistance of soil against erosion, to reduce runoff and increase infiltration, to reduce speed of runoff, to drain runoff and to increase the roughness of the

ground surface (Feng, 1995; Osman, 2014). Methods of soil erosion can be classified into three categories: agronomic, biological and physical.

Physical measures are structures built to increase the time of concentration, divide long slopes into short ones and reduce velocity of surface runoff. Some physical measures include terraces, bunds, check dams, contour ditches, grassed waterways and retention reservoirs. Biological measures work to provide protection against impact of rainfall. They prevent splash erosion, reduce velocity of surface runoff, enhance accumulation of soil particles and stabilize soil aggregates. Some of the measures include vegetative strips and afforestation. Agronomic measures intercept raindrops to reduce their impact on soil surface and as a result reduces soil erosion on. They also increase infiltration and reduce surface runoff. Some agronomic measures are strip cropping, mixed cropping, intercropping, agroforestry, contour ploughing, mulching, grazing management, fallowing, crop rotation, conservation tillage.

The estimated global rate of soil erosion by water is 20 to 30 gigatonnes per year. The rate translates to local averages of 10 to 20 tonnes per hectare per year and local peaks of 50 to 100 tonnes per hectare per year. On the other hand, soil formation rate is estimated to be 1 tonne per hectare per year (FAO, 2015). The big difference in rate of soil erosion and rate of soil formation makes soil a non-renewable resource, considered over human time-scale (Blanco-Canqui and Lal, 2010; FAO, 2015). In the humid and sub-humid zones of Sub-Saharan Africa, the estimated average annual soil loss to water erosion is 50 tonnes per hectare. The high rate is attributed to deforestation, heavy rainfall (Obalum *et al.,* 2012) and extensive expansion of agricultural land.

In Kenya, about 30 per cent of the land is degraded and an estimated 12 million people live on the degraded land. The cost of land degradation is about 1.3 billion United States Dollars (USD) per year (Mulinge *et al.,* 2015). Soil erosion is the main physical agent of land degradation (GoK, 2013). The annual loss of soil to water erosion is about 72 tonnes per hectare and this has led to about 20 per cent irreversible loss in productivity (Mulinge *et al.,* 2015*)*. In tropical countries, pressures on soil erosion include intense rainfall, highly erodible soils, removal of land cover and inappropriate soil management practices (Wantzen and Mol, 2013). Deforestation and land cultivation can cause an increase in temperature, conductivity, total suspended and dissolved solids and turbidity of water (Kasangaki, Chapman, and Balirwa, 2008). Several catchment studies have shown that there is a strong correlation between concentrations of nutrients in river water and the

percentage of catchment land under agriculture (Stålnacke, Grimvall, Libiseller, Laznik, and Kokorite, 2003).

In Kenya, most catchments are characterized by deforestation, human settlements, reclamation of wetlands and unsustainable agricultural activities (Aura, Raburu and Herrmann, 2011; Ontumbi, Obando and Ondieki, 2015). In River Nzoia catchment in western Kenya, human activities have led to extensive change in land use, hydrology and water quality. For instance, Twesigye, Onywere, Getenga, Mwakalila and Nakiranda (2011) observed high levels of nitrates and phosphates along the agricultural zones of the catchment. In another study by Maloba, Khaemba, Njenga and Akali (2016) to establish the effects of increased land use change on runoff and sediment yield in the upper Nzoia catchment, the runoff coefficient for the area increased from 44% in the year 2000 to 51% in the year 2014. It also revealed that the annual sediment yield increased from 1400.79 tonnes in the year 1990 to 1967.46 tonnes in the year 2014. In addition, the study showed that the predicted annual sediment yield will be 3592.07 tonnes in the year 2020 and 3767.90 in the year 2030.

Sosiani catchment is part of the upper River Nzoia drainage area. Sosiani river is one of the sources of water in Uasin Gishu County and Eldoret town in Kenya. Between 1973 and 2013, the catchment underwent huge land cover changes. Forest cover decreased from 109 km^2 to 43 km^2. Farmlands expanded from 102 km^2 to 486 km^2. Grasslands decreased from 430 km^2 to 46 km^2 while the urban area grew from 2.5 km^2 to 68 km^2. The land use change had profound impact on runoff (Barasa, 2014). In another study, Ontumbi *et al.* (2015) noted that the impact of agricultural activities in Sosiani catchment could be seen in changes in water quality parameters from upstream to downstream along River Sosiani. They observed an increasing trend in temperature, total phosphates, nitrates, pH, turbidity, electrical conductivity and total suspended solids. In their recommendations, Barasa (2014) advised that forest conservation, agroforestry and adoption of sound agricultural practices would help to reduce soil erosion and increase the lag time of flow in the catchment and Ontumbi *et al.* (2015) recommended that that all development and land use activities in Sosiani catchment need to consider ecological integrity.

1.2 Statement of the Problem

The increasing trend in temperature, total phosphates, nitrates, pH, turbidity, electrical conductivity and total suspended solids from upstream to downstream along River Sosiani

(Ontumbi *et al.,* 2015) is a manifestation of the impact of land use change on the hydrology of Sosiani catchment. The impact of land use change in a river catchment is usually driven by various hydrological relationships. In the context of Sosiani catchment, key is the relationship between rainfall, runoff, soil erosion and sediment yield. This study seeks to explore the use of a physically-based distributed hydrologic model to simulate the relationship between rainfall magnitude, runoff, soil erosion and sediment yield under different management scenarios in Sosiani catchment. The results will be used to formulate the best options for sustainable management of the catchment.

1.3 Objectives

1.3.1 Broad Objective

The broad objective of the study was to model the effect of rainfall magnitude on runoff, soil erosion and sediment yield in Sosiani catchment with a view to providing the best conservation practices.

1.3.2 Specific Objectives

i. To simulate effect of rainfall on spatially distributed runoff in Sosiani catchment for the period 1994 to 2014.

ii. To determine the effect of rainfall on spatially distributed soil erosion in the catchment for the same period.

iii. To simulate effect of rainfall on spatially distributed sediment yield for different management scenarios.

iv. To formulate the best soil and water conservation and management options for the catchment.

1.3.3 Research Questions

i. What is the relationship between rainfall magnitude and spatially distributed runoff in Sosiani catchment?

ii. How does rainfall magnitude influence spatially distributed soil erosion in Sosiani catchment?

iii. How would rainfall magnitude affect sediment yield in Sosiani catchment under different management scenarios?

iv. What is the most appropriate soil and water conservation strategy for Sosiani catchment?

1.4 Justification of the Study

Existing studies indicate that land use change and soil erosion has profound impact on hydrology and surface water quality in the catchment. However, there is inadequate information regarding the extent of soil erosion and sediment yield in the catchment. The results of this study are intended for a multi-user audience consisting of users from policy, development, agriculture, water, education, research and administration sectors. It will help to understand the spatio-temporal trends in distribution of runoff, erosion and sediment yield within the catchment. It will facilitate assessment of effectiveness and efficiency of erosion control practices and inform policy and practice on soil and water conservation, sustainable agriculture and catchment investment planning.

1.5 Scope and Limitations of the Study

The study aimed to formulate the best soil and water conservation strategy for Sosiani catchment in the upper River Nzoia drainage area in Kenya. Soil and Water Assessment Tool within an Arc GIS environment (Arc-SWAT) was used to spatially simulate the effect of rainfall magnitude on runoff, soil erosion and sediment yield in the catchment on a monthly time-step for the period 1994 – 2014. The datasets included both observed and satellite-derived data. Limitations that the study faced include data related limitations such as short time series, errors, missing data; time limitations such as inadequate time to ground-truth satellite derived products and model results; and financial limitations such as inadequate funds to acquire observed data from relevant agencies and/or carry out field measurements

CHAPTER TWO

LITERATURE REVIEW

 2.1   Soil Erosion

This section comprises a brief discussion of mean soil loss tolerance value, classes of soil erosion, factors influencing soil erosion, systematic approach to erosion management, need for erosion modelling, basic equations used in hydrologic and erosion models and physically based soil erosion-sediment models.

2.2.1   Mean Soil Loss Tolerance Value

Soil erosion is an important process in landscape sculpture and soil formation. However, excess of soil erosion, usually beyond a tolerable level, can adversely affect productivity of the land, quality of water, functioning of riparian communities and performance of water infrastructure. The mean soil loss tolerance value or level is the magnitude of soil erosion beyond which productivity is adversely affected (Borah, Krug, and Yoder, 2008; Blanco-Canqui and Lal, 2010). The value varies with farming systems, land cover, ecology and topography and it is important in soil and water conservation planning (Blanco-Canqui and Lal, 2010).

2.2.2   Gross Soil Erosion

The total amount of soil lost from a catchment due to erosion is referred to as gross soil erosion. A fraction of this amount usually does not reach the outlet point of interest within the catchment.

2.2.3   Classes of Soil Erosion

Erosion can be classified as natural or human-induced or according to the erosive agents. Based on the erosive agent, the classes are water erosion and wind erosion. This study shall focus on water erosion, which involves detachment and transport of soil particles by water to a point remote from the source. The sub-classes of water erosion are splash erosion, inter-rill and rill erosion, sheet erosion, gully erosion and streambank erosion (Osman, 2014).

2.2.4   Factors Influencing Soil Erosion

According *to* (Blanco-Canqui and Lal, 2010), soil erosion is usually accelerated by three main drivers: overgrazing, deforestation and mismanagement of cultivated lands. The factors that

influence water erosion include soil properties, land and vegetative cover, climate and topography (Morgan, 2005; Blanco-Canqui and Lal, 2010; Rhode Island State Conservation Committee, 2014) and dewatering activities (Rhode Island State Conservation Committee, 2014). A fifth factor that depends on the four is runoff erosivity.

Climatic factors include precipitation, temperature, humidity, solar radiation, evapotranspiration and wind velocity. Rainfall erosivity usually depends on depth or amount of rainfall, terminal velocity of raindrops, rainfall intensity and the size of the raindrops. Runoff erosivity depends on runoff volume, time of concentration, peak runoff rate and characteristics of the hydrologic group. Topographic factors include size and shape of the catchment (Borah *et al.,* 2008)*,* the size, degree and length of the slope (Morgan, 2005; Blanco-Canqui and Lal, 2010). Soil properties affecting soil erodibility include structure, texture; aggregate, strength, stability, density and wettability, antecedent soil water content, macroporosity, soil infiltration, soil organic matter content, saturated hydraulic conductivity (Blanco-Canqui and Lal, 2010) and clay mineralogy (Borah *et al.,* 2008).

### 2.2.5   Systematic Approach to Soil Erosion Management

A typical systematic approach to erosion control involves measurement, modelling and management *(*Owens and Collins, 2006). To measure is to identify and quantify rate, magnitude, severity, timescale, impact, sources, pathways and sinks of erosion and sediment. To model is to understand, predict and simulate trends and patterns of the phenomenon. Models can be empirical, process based or physically based (Morgan and Nearing, 2011), conceptual and stochastic. Modelling usually requires reliable spatio-temporal data. To manage is to identify the problem, quantify its impact, execute a control solution and assess the performance of the solution. The process, its evaluation and modification rely on measurement and modelling outcomes. Typical management options include control of the source, interception, retention and remediation. Figure 2.1 represents the systematic approach. It is adapted from Owens and Collins (2006) and modified.

2.2.6   Need for Erosion Modelling

Describing erosion rate in the whole catchment over space and time is a challenge because of limited field measurements for every part of the catchment. In conservation studies, there is usually

a need to investigate how rates of erosion respond to changes in land use and climate (Pandey, Himanshu, Mishra, and Singh, 2016a). In addition, the effectiveness and efficiency of erosion control measures also needs to be studied. The studies usually need detailed field data collected over a long period of time. Such measurements are usually costly. In addition, most environmental problems need to be solved immediately as opposed to many years needed for field data measurements (Morgan and Nearing, 2011).

Figure (2.1). An overview of systematic erosion control
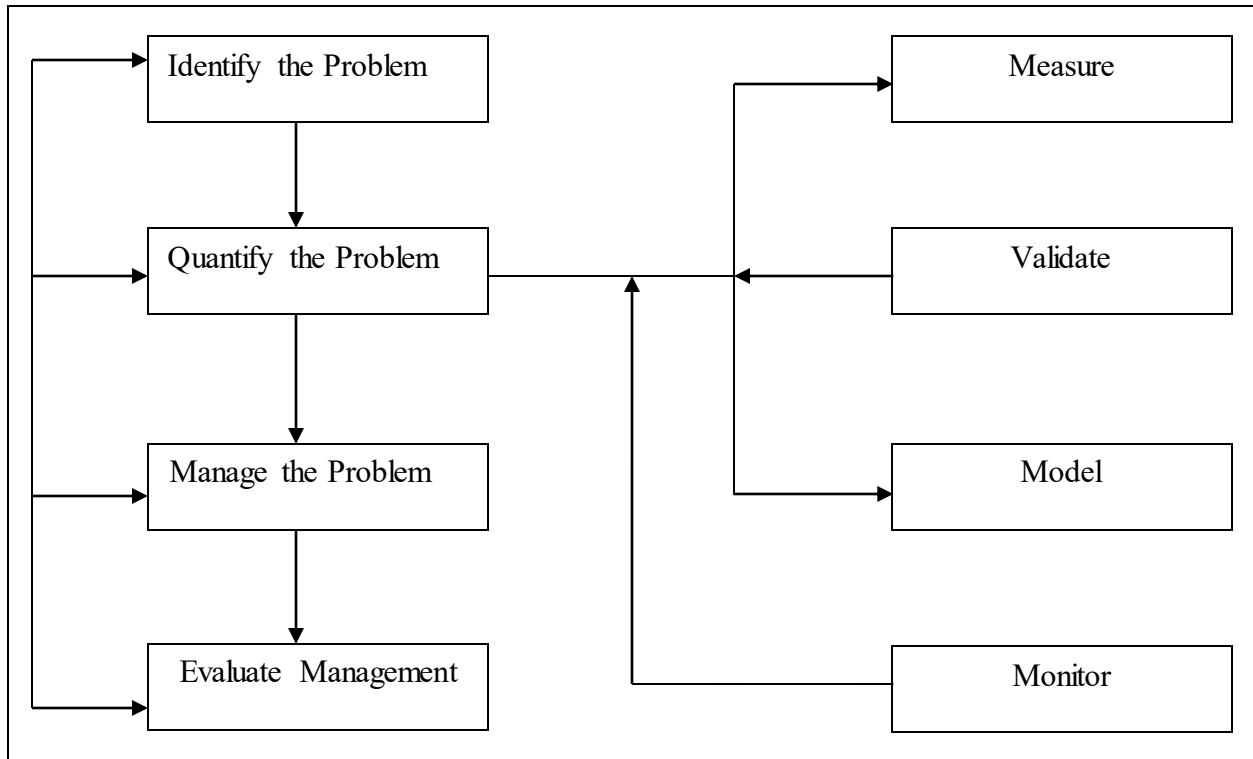
Models can be applied satisfactorily to solve the difficulty by simulating and predicting erosion over a range of scenarios (Morgan and Nearing, 2011; Pandey *et al.,* 2016a). However, since a model is a simplification of reality, there is a drawback of uncertainty and error in every modelling process. An erosion model will be close to reality if it is applied to conditions for which it is calibrated and validated (Morgan and Nearing, 2011).

2.2.7 Basic Equations Used in Hydrologic, Erosion and Sediment Models

Equations used in most hydrologic and erosion models fall in four broad categories. They include water balance equations, flow governing equations, sediment yield equations and routing equations.

2.2.7.1 Water Balance Equations

Water balance equations are used for hydrologic water accounting. An example of the equation is the land phase hydrologic cycle water balance equation (Neitsch, Arnold, Kiniry, and Williams Grassland, 2011a).

$$SW_t = SW_0 + \sum_{i=1}^{t} \left(R_{day} - Q_{surf} - E_a - w_{seep} - Q_{gw} \right) \tag{2.1}$$

Where:

SW_t = final soil water content (mm),

SW_0 = initial soil water content (mm),

t = time (days),

R_{day} = amount of precipitation on the day i (mm),

Q_{surf} = accumulated surface runoff or excess precipitation on the day i (mm),

E_a = amount of evapotranspiration on the day i (mm),

w_{seep} = amount of water entering the vadose zone from the soil profile on the day i (mm),

Q_{gw} = amount of return flow for the day (mm).

2.2.7.2 Flow Governing Equations

Flow governing equations are used to estimate runoff or excess precipitation. The following are examples of the equations:

Kinematic wave equation (Saint-Venant, 1871; American Society of Civil Engineers, 1996; Pandey *et al.,* 2016):

$$\frac{dh}{dt} + \frac{dQ_{surf}}{dx} = q \qquad \text{when} \quad S_0 = S_f \tag{2.2}$$

Where:

h = depth of flow (m),

Q_{surf} = runoff or flow (m³ s⁻¹),

t = time (s),

q = flow per unit width (m³ s⁻¹ m⁻¹),

S_0 = bed or surface slope (m m⁻¹),

S_f = energy gradient (m m⁻¹).

Manning's equation (Manning, 1891; Wilson, 1969; Swamee and Chahar, 2015; Pandey *et al.,* 2016a)*:*

$$Q_{surf} = \frac{1}{n} A R^{\frac{2}{3}} S_0^{\frac{1}{2}}$$ (2.3)

Where:

Q_{surf} = runoff or flow (m³ s⁻¹),

A = flow area (m²),

R = hydraulic radius (m),

S_0 = bed or surface slope (m m⁻¹).

Soil Conservation Service Curve Number (Mishra and Singh, 2003; Hawkins, 2009). It is abbreviated as SCS-CN:

$$Q_{surf} = \frac{\left(R_{day} - I_a\right)^2}{\left(R_{day} - I_a + S\right)}$$ (2.4)

Where:

Q_{surf} = surface runoff in (mm),

I_a = initial abstraction including surface storage, interception and infiltration before start of runoff (mm),

R_{day} = precipitation depth for the day (mm),

S = the retention parameter (mm).

When $I_a \cong 0.2S$ equation 2.5 becomes:

$$Q_{surf} = \frac{\left(R_{day} - 0.2S\right)^2}{\left(R_{day} + 0.8S\right)}$$ (2.5)

$$S = 25.4 \left(\frac{1000}{CN} - 10\right)$$ (2.6)

CN = curve number for the day.

Modified Rational Formula (Neitsch *et al.,* 2011a)*:*

$$q_{peak} = \frac{\alpha_{tc} \times Q_{surf} \times A}{3.6 \times t_{conc}}$$

(2.7)

Where:

q_{peak}= peak runoff rate in ($m^3 s^{-1}$),

α_{tc} = fraction of daily rainfall that occurs during time of concentration in (mm),

t_{conc} = time of concentration for the sub-basin in (hr.),

A = the area of the sub-basin (Km^2),

3.6 = unit conversion factor,

Q_{surf} = surface runoff as defined in equation 2.5.

2.2.7.3 Hillslope Sediment Yield Equations

Sediment yield equations are used to estimate the amount of eroded soil that is delivered to an outlet point from a catchment. The following are examples of the equations:

Revised Universal Soil Loss Equation (Renard, Foster, Weesies, and Porter, 1991). It abbreviated as RUSLE:

$$E = R_{usle} \times K_{usle} \times L_{usle} \times S_{usle} \times C_{usle} \times P_{usle}$$

(2.8)

Where,

E = average annual soil loss (tonnes ha^{-1} yr^{-1}),

R_{usle} = rainfall erosivity factor (MJ ha^{-1} mm^{-1}),

K_{usle} = soil erodibility factor (tonnes ha^{-1} yr^{-1}),

L_{usle} = slope factor (m),

S_{usle}= slope steepness factor (degrees),

C_{usle} = crop management factor (no units),

P_{usle} = conservation practice factor (no units).

Modified Universal Soil Loss Equation (Williams and Berndt, 1977a)**.** It is abbreviated as MUSLE.

$$sed = a\left(Q_{surf} \times q_{peak} \times A_{hru}\right)^b K_{usle} \times C_{usle} \times P_{usle} \times LS_{usle} \times CFRG$$

(2.9)

Where,

sed= the sediment yield on a given day (metric tonnes),

Q_{surf} = the surface runoff ($mmha^{-1}$),

q_{peak} = the peak runoff rate (m^3s^{-1}),

A_{hru} = area of the hydrologic response unit (ha),

LS_{usle} = topographic factor,

CFRG = coarse fragment factor,

a and b = coefficients.

Generally, a = 11.8 and b = 5.6.

Foster Equation (Foster, Meyer, and Onstad, 1977):

$$\frac{dq_s}{dx} = D_i + D_r \tag{2.10}$$

Where,

$\frac{dq_s}{dx}$ = sediment rate per unit width of rill channel,

D_i = rill net detachment,

D_r = inter-rill net detachment.

2.2.7.4 Flow Routing Equations

Flow routing equations are used to characterize movement of flow downstream in a channel. An example is the Muskingum Routing Method (Chen and Liew, 2003, p.1137).

2.2.7.5 Sediment Routing Equations

Sediment routing equations are used to characterize movement of sediment downstream in a channel. An example is Bagnold's Stream Power Equation (Bagnold, 1977):

$$Conc_{sed,ch,max} = C_{sp} \times V_{ch,pk}^{spexp} \tag{2.11}$$

Where,

$Conc_{sed,ch,max}$ = the maximum concentration of sediment that can transported by water (tonnes m^{-3}),

C_{sp} = user-defined coefficient,

$V_{ch,pk}$ = is peak channel velocity (ms^{-1}),

spexp = user-defined coefficient, usually between 1.0 and 2.0 (Neitsch *et al.,* 2011a).

$$sed_{out} = sed_{ch} \left(\frac{V_{out}}{V_{ch}}\right) \tag{2.12}$$

Where,

sed_{out} = amount of sediment transported out of reach (metric tonnes),

sed_{ch} = amount of suspended sediment in the reach (metric tonnes),

V_{out} = volume of outflow during the time step (m^3 of water),

V_{ch} = volume of water in the reach segment (m^3 of water).

2.2.8   Basic Data Used in Hydrologic, Erosion and Sediment Models

Basic data used in hydrologic, erosion and sediment models include digital elevation model (DEM), soil data, land use/land cover (LULC) data, weather data, river flow data, sediment data, groundwater data and observation location data.

Digital Elevation Model (DEM) Data

In hydrologic, erosion and sediment yield modelling, the digital elevation model is used to delineate and sub-divide the catchment into sub-catchments. It is also used together with land use and soil data to divide the catchment into hydrologic response units (HRUs). Sub-basin parameters used to describe the morphometric character of the catchment are derived from the digital elevation model. The quality of the digital elevation model usually influences the quality of the output of the hydrological model (Lowell and Jaton, 1999). The resolution of the digital elevation model is an important parameter (Gassman, Reyes, Green, and Arnold, 2007) because it influences delineation of the catchment, generation of channel network, classification of sub-catchments and the number of sub-catchments and hydrologic response units. Sediment yield simulation and prediction is usually sensitive to the number and size of sub-catchments and hydrologic response units (Jha, Gassman, Secchi, Gu, and Arnold, 2004). Moreover, Chaubey, Cotter, Costello, and Soerens (2005) established that the resolution affects the total area of the delineated catchment. A low resolution would result into a large error in the predicted runoff and sediment.

The number, scale and size of sub-catchments usually influence the process and results of catchment modelling (Jha *et al.,* 2004). When the number of sub-catchments is increased, data preparation effort and computational evaluation increase but when the number is decreased, simulation results may be affected. In addition, streamflow simulation is less affected by the number of sub-catchments while sediment simulation is sensitive to the size of the sub-catchments. Scaling affects the geometric properties of the sub-catchments and consequently the simulation of hydrologic variables. For instance, the total length of streams per unit area, also called drainage

density, affects runoff. Therefore, appropriate catchment size and scale thresholds usually need to be established so as to achieve efficient and adequate simulation of the catchment. For instance, according to Jha *et al.* (2004), the appropriate area of the smallest subcatchment can be 3 percent of the total catchment area.

Currently in Kenya, 30-meter DEM is the finest or highest resolution available to the public on open access. Two commonly used DEMs are the Advanced Space borne Thermal Emission and Reflection Radiometer (ASTER) Global DEM (Abrams, 1999) and the Shuttle Radar Topography Mission (STRM) global DEM (Farr *et al.,* 2007). According to Forkuor and Maathuis (2012), the STRM DEM has a better accuracy than that of ASTER DEM with reference to how close the estimation is to a reference DEM. The STRM DEM overestimates elevation. The overestimation can partly be explained by the fact that STRM records the reflective surface and in the presence of vegetation, it may be positively biased with reference to the bare ground. The ASTER DEM underestimates elevation. The underestimation is higher on flat and less complex terrains as is on hilly complex terrains.

Soil Data

Soil data is used to determine the water budget in the soil profile, runoff and erosion. It affects catchment water balance by influencing processes such as infiltration, percolation, ponding, runoff and storage. The processes are influenced through soil properties such as erodibility factor, infiltration capacity, hydraulic conductivity among others. In some hydrologic modelling activities, the surface and upper subsurface of the catchment is usually described in the soil database. The database represents the soil and the coupled soil characteristics in the study area. The characteristics constitute textural and physico-chemical properties of the soil layers.

The resolution of soil data is important because it influences the number of hydrologic response units. A low resolution may assign a single classification to an area that would have more soil types if a dataset with higher resolution was to be used. Such generalization affects the slope and the slope length of the hydrologic response units and consequently the sediment yield (Geza and McCray, 2008). In simulation studies, large differences in simulated surface water flow and ground water recharge can be caused by resolution of the soil dataset. The differences in flow and recharge can lead to significant difference in simulated sediment. The difference in simulated sediment yield and related water quality parameters can have an impact on the design, implementation and outcome of conservation practice (Moriasi and Starks, 2010).

The Harmonized World Soil Database (HWSD) version 1.2 is the latest and highest resolution soil database with high reliability available to the public on open access in Eastern Africa. It has a resolution of 1kilometre (30 arc seconds by 30 arc seconds), with 221 million grid cells that cover the entire earth land surface. It has 16000 mapping units which are linked to a harmonized attribute database. The database has a standardized structure that allows linking attribute data to ArcGIS. The linkage allows for querying and characterization of the soil. Content of the database is categorized into three blocks. The blocks include general information on the soil mapping unit component, information related to phases, physical and chemical characteristics of topsoil (0-30cm) and sub-soil (30-100cm) (FAO/IIASA/ISRIC/ISS-CAS/JRC, 2009).

Land Use/Land Cover Data

Land use and land cover influence runoff, infiltration, evapotranspiration, erosion and sediment yield in the catchment. Some hydrologic, erosion and sediment models use land cover information, soil information and slope information to estimate curve numbers for estimation of runoff.

Weather Data

Weather data includes rainfall, air temperature, solar radiation, wind speed and relative humidity and evapotranspiration. The data is useful in simulating the water budget of the catchment.

Flow Data

This comprises river flow gauging data at a point (for single site simulation) or specific points (for multi-site simulation) in the river network within the catchment. Observed flow data is usually used to calibrate and validate model runoff simulations. It can also be used together with turbidity data to generate sediment data in catchments where sediment data is non-existent or limited.

Sediment Data

Observed sediment data is used calibrate and validate model simulations of sediment yield. In cases where sediment data is missing, a surrogate method can be used to generate the data. For instance, turbidity data can be used as surrogate for suspended-solids concentrations (Wass and Leeks, 1999; Minella, Merten, Reichert, and Clarke, 2008). The method involves establishing a regression equation between turbidity and suspended solids concentrations. According to Umit (2015), the total suspended solids loadings can be calculated as the product of flow and suspended solids concentrations:

$$\text{Sed}_{\text{total}}=0.864\times Q_{\text{surf}}\times C_{\text{sed}} \tag{2.13}$$

Where,

$\text{Sed}_{\text{total}}=$ sediment discharge (tons day^{-1}),

$Q_{\text{surf}}=$ surface runoff (m^{3}s^{-1}),

$C_{\text{sed}}=$ sediment concentration (ppm) or (mgl^{-1}).

$0.864=$ conversion factor.

A similar method by Post and Jakeman (1996) was used by Maloba *et al.* (2016) in Nzoia river basin:

$$\text{Sed}_{\text{total}}=0.0864\,(1.41t+1.917)\,Q_{\text{surf}} \tag{2.14}$$

Where,

$\text{Sed}_{\text{total}}=$ sediment discharge (tons day^{-1}),

$Q_{\text{surf}}=$ surface runoff (m^{3}s^{-1}),

$t=$ turbidity of water (NTU),

$0.0864=$ conversion factor,

1.4 and $1.917=$ empirical constants

2.2.9 Physically Based Soil Erosion-Sediment Models

Physically based spatially distributed models satisfactorily simulate or predict output at a desired location within a catchment (Pandey *et al.,* 2016a). They are used to identify critical or priority erosion and sediment yield areas. They are also used to evaluate and simulate soil and water conservation practices at a low cost. The next section is a summarized description of three physically based erosion models. The following is a summarized description of three physically based erosion models.

Water Erosion Prediction Project (WEPP) Model

WEPP is both lumped and distributed continuous and event-based field and catchment model able to simulate both channel and hillslope sediment. It has moderate potential to integrate

with GIS. It was developed by Laflen, Lane, and Foster (1991). Input variables include climate, soil, topography, cultural practices, channel, impoundment (Laflen *et al.,* 1991). It uses Foster Equation to model soil erosion and sediment yield. It can model runoff; soil erosion and sediment yield on an event or continuous basis using daily time step.

The advantage of WEPP is that it can simulate most of the physical processes necessary for soil erosion modelling (Pandey *et al.,* 2016a). The processes include runoff, infiltration, sediment transport, sediment deposition, plant growth and residue decomposition. Several studies have used WEPP in water erosion and sediment yield modelling and implementation of best catchment management practices (Raclot and Albergel, 2006; Pandey, Chowdary, Mal, and Billib, 2008; Defersha, Melesse, and McClain, 2012). However, its shortcoming is that it requires a large number of input data and model parameters. In addition, it is unable to simulate the processes occurring in permanent channels such as perennial streams and classical gullies (Pandey *et al.,* 2016a).

Annualized Agricultural Non-Point Source (AnnAGNPS) Model

It is a distributed continuous catchment model able to model channel and hillslope sediment. It has high potential to integrate with GIS. Version 5.45 released in 2016 is was developed by Bingner, Theurer, and Yuan (2015). Its governing equations for soil erosion and sediment yield modelling are Revised Universal Soil Loss Equation, Bagnold transport equation and modified Einstein deposition equation (Bingner *et al.,* 2015; Pandey *et al.,* 2016a). It can be used to simulate, on a daily or sub-daily time-step, nutrient transport, sediment yield and hydrology over a long period of time. It is a good Tool for comparison of effectiveness of catchment conservation practices. Several studies have used AnnAGNPS to runoff; sediment yield (Shrestha, Babel, Das Gupta, and Kazama, 2006; Licciardello, Zema, Zimbone, and Bingner, 2007; Yuan, Locke, and Bingner, 2008; Bisantino, Bingner, Chouaib, Gentile, and Trisorio Liuzzi, 2015).

However, the limitation is that all runoff and sediment load for a single daily event are routed to the catchment outlet before the next day simulation (Bingner *et al.,* 2015). In addition, the model requires extensive input data and lacks mass balance calculations (Pandey *et al.,* 2016a).

Soil and Water Assessment Tool (SWAT) Model

The soil and water assessment Tool (SWAT) is a physically based, semi-distributed, continuous, catchment scale simulation model (Neitsch, Arnold, Kiniry, and Williams Grassland,

2011b; Pandey, Himanshu, Mishra, and Singh, 2016b). The model requires data on weather and climate, soil, topography, land use including land cover and management practice as input for hydrologic, soil erosion, sediment yield, nutrient and conservation practice simulation in large complex catchments (Neitsch *et al.,* 2011b; Pandey *et al.,* 2016b). The physically-based approach enables users to model ungauged catchments and quantify the relative long-term impact of alternative input data on various variables on interest. In addition, the model is computationally efficient and has a low minimum data requirement (Neitsch *et al.,* 2011b).

SWAT categorizes the input variables into hydrologic response units abbreviated as HRUs. The units are lumped land areas in the sub-basin, which have exclusive combinations of land cover, soil and management, climate, wetlands, groundwater and reach. The water balance equation is used to represent the catchment. It is divided into the land phase and the routing phase. The land phase controls amount of water, sediment and nutrient loads to the main channel in each sub-basin, while the routing phase controls the movement of these loads in the channels to the outlet of the catchment (Neitsch *et al.,* 2011b).

The model uses daily or sub-daily rainfall input to simulate overland flow magnitudes and peak rates (Neitsch *et al.,* 2011b) based on either the SCS-Curve Number method (Mishra and Singh, 2003) or the Green and Ampt Infiltration Method (Green and Ampt, 1911). The curve number method is unable to directly model infiltration, therefore, the amount of water that enters the soil profile is estimated as the difference between the magnitude of rainfall and the magnitude of surface runoff while the peak runoff rate is simulated using Modified Rational Method and sub-basin time of concentration estimated using the Manning's Equation (Neitsch *et al.,* 2011b*).*

The SWAT model simulates transmission loses using Lane's Method (Natural Resources Conservation Service, 1983) and evapotranspiration using by either Hargreaves Method (Hargreaves, Hargreaves, and Riley, 1985) or Penman-Monteith Method (Monteith, 1965) or Priestley-Taylor Method (Priestley and Taylor, 1972). Erosion and sediment yield are simulated using the Modified Universal Soil Loss Equation (Williams and Berndt, 1977). Flow routing is based on William's Variable Storage Coefficient Method (Williams, 1969) or Muskingum Routing Method (Chen and Liew, 2003) while sediment routing is based on Bagnold's Stream Power Concept (Bagnold, 1977b).

SWAT can be applied in complex catchments and catchments that are ungauged or have limited data. Several studies have used SWAT to study runoff, soil erosion and sediment yield as well as to develop strategies for catchment conservation (Arabi, Frankenberger, Engel, and Arnold, 2008; Hunink, Niadas, Antonaropoulos, Droogers, and de Vente, 2013a; Mwangi, Shisanya, Gathenya, Namirembe, and Moriasi, 2015a; Adeogun, Sule, and Salami, 2016; Ben Salah and Abida, 2016a).

In a study of Corbeira, rural catchment covering an area of 16 km^2 in northwestern Spain, Rodríguez-Blanco *et al.* (2016) tested the applicability of SWAT to simulate sediment yield in the catchment. The model predicted a mean annual sediment yield of 0.105 tonnes ha^{-1} yr^{-1} while the observed was 0.11 tonnes ha^{-1} yr^{-1}. They established that cultivated land contributed 79% of the sediment yield. They concluded that the model was applicable to simulate sediment yield in the catchment but had the tendency to underestimate sediment yield in wet months and overestimate in the dry months. The performance evaluation values for calibration and validation respectively were 0.67 and 0.84 for coefficient of determination (R^2), 6% and 12% for percent bias (PBIAS) and 0.48 and 0.50 for Nash-Sutcliffe Efficiency (NSE). They calibrated and validated the model for monthly time step using observed sediment yield (2005-2010). The catchment was covered by forest (65%), agricultural area (30% with 4% cultivated) and built up area (5%). It had annual rainfall of 1050 mm and evaporation of 620 mm. It had low surface runoff and high base flow. The study indicated that even though SWAT is developed for application in large catchments, it gives satisfactory results in small catchments with good quality input data.

In another research, (Ben Salah and Abida, 2016) used SWAT to simulate daily and monthly flow and sediment magnitudes in 2200 km^2 Wadi Hatab catchment in central Tunisia. The sediment yield values during calibration and validation were 1.15 and 5.37 tonnesha^{-1}year^{-1} respectively. They concluded that SWAT satisfactorily models flow and sediment yield in the catchment but tends to underestimate flow peaks. Performance evaluation gave values of 0.52 and 0.61; 0.54 and 0.61 for Nash-Sutcliffe Efficiency (NSE) and the coefficient of determination (R^2) respectively for calibration and validation at daily time-step.

For the monthly time-step, the values were 0.67 and 0.89 for NSE and 0.83 and 0.87 for R^2 for calibration and validation respectively. They calibrated and validated the model using flow data due to lack of sediment data. They argued that since sediment yield depends on soil, land use and

flow input, a good simulation of flow would give a reasonable estimate of sediment yield. The study area was characterized by fragile soils, abrupt topography and significant contrast in climate and mixed land-cover with forests (33.2%) and range bushes (34.7%). This study demonstrated the ability of SWAT model to use readily available data to give reliable output in ungauged catchments. However, lack of observed sediment data for model calibration and validation could be a source of uncertainty in the results from the study.

In Kenya, Hunink, Niadas, Antonaropoulos, Droogers, and de Vente (2013) used SWAT to identify intervention areas to reduce reservoir sedimentation in Tana catchment (9500 km^2). They concluded that SWAT was applicable to model spatial variability of erosion and sediment yield in Tana catchment. The model simulated 80% of the observed sediment yield. The main sediment sources were located on steep slopes. Coffee planted areas had erosion rates of about 50 tonnes ha^{-1} yr^{-1}. Maize and tea planted areas had erosion rates of about 10 tonnes ha^{-1} yr^{-1}. They calibrated and validated the model using observed rainfall and sediment data.

For validation of water flows, Nash-Sutcliffe Efficiency (NSE) value was 0.75. Percent bias (PBIAS) value was -9%. Standard deviation of the Root Mean Square Error (RSR) was 0.50. The coefficient of determination of the (R^2) for simulated sediment loads was 0.95. The annual rainfall ranged between 2000 mm at the higher altitudes and 500 mm at the lower altitudes. The area had potential annual evapotranspiration of 1000 mm. Rainfed subsistence agriculture constituted 60% of the land use. In the study, tea planted areas had high erosion rates in spite of the dense canopies of tea farms. These high erosion rates could be attributed to steep slopes on which tea farming is done in Tana catchment. Temporal land use data was not used in the study. The study did not simulate spatio-temporal trends in land use and their relationship with erosion. These trends are useful in characterizing the watershed for conservation interventions. The study showed that Sasumua sub-catchment, within the larger Tana catchment, had sediment yield of less than 0.2 tonnes ha^{-1} yr^{-1}.

However, in a different study, Mwangi, Shisanya, Gathenya, Namirembe and Moriasi, (2015) simulated sediment yield of 3.8 tonnes ha^{-1} yr^{-1} from the catchment using SWAT Model. This discrepancy creates a need for re-examination of the two studies. However, the studies illustrate that, SWAT model is applicable to a range of watershed conditions but has the tendency to underestimate high flows and overestimate low flows. A good time series of observed data and

sound hydrologic intuition are usually desirable so as to make a good interpretation of the model output.

SWAT Calibration and Uncertainty Programs (SWAT-CUP)

SWAT-CUP is a computer program developed and used for sensitivity analysis, calibration, validation and uncertainty analysis of SWAT models (Abbaspour, 2015). Sensitivity analysis involves determining a change in model output variable values that result from a change in model input variable values. It is an inquiry of the importance of imprecision or uncertainty in model inputs in a modelling or decision-making process (Loucks, Beek, and Stedinger, 2005). There are two approaches to sensitivity analysis: global sensitivity analysis and one-at-a-time sensitivity analysis. In global sensitivity analysis, a group of parameters are varied at the same time while one-at-a-time sensitivity analysis is performed on one parameter at a time only (Abbaspour, 2015b). One of the areas of focus in sensitivity analysis is to estimate general uncertainty associated with model predictions so that policy decisions can reflect both the modelling efforts' best prediction of system performance and the precision of such predictions (Loucks *et al.,* 2005). It can be used to analyze both model and system performance.

Uncertainty analysis describes a whole set of possible model outcomes as well as their associated probabilities of occurrence. It involves comprehensively identifying all sources of uncertainty that contribute to the joint probability distributions of each input or output variable. Uncertainty can be categorized into knowledge uncertainty and decision uncertainty (Loucks *et al.,* 2005), parameter, structural and data uncertainty (Gupta, Beven and Wagener, 2005). Uncertainty analysis can be used to estimate the probability that the model output will exceed a certain limit or threshold or performance measure target value; assign a reliability level to function of the outputs and estimate the relative impact of input variable uncertainties (Loucks *et al.,* 2005).

Modelling is a simplification of reality. To represent the reality as close as possible, model parameters are adjusted and estimated to obtain a match between observed and simulated catchment behavior. The process is called model calibration. The purpose of model calibration is to obtain a model with the following attributes: (i) the structure and behavior of the model obey the current hydrologic understanding of reality, (ii) the model input-state-output behavior is consistent with catchment behavior measurements, (iii) model simulations and predictions have negligible bias and relatively small prediction uncertainty (Gupta *et al.,* 2005). Calibration

approaches can either be manual, automated or a combination of both. Manual calibration is an intuitively guided trial and error approach in which the modeler's understanding of the model and how each parameter affects the output are used to guide changes to parameter values. Decisions regarding which parameter values to modify are made by graphical comparison of simulated and observed values. Automated calibration approach uses computer algorithms to best simulate observed values. Values of user specified parameters are varied to achieve an optimal fit. Decisions are made based on single or multiple statistical objective functions.

Model validation is the demonstration that the model represents or reproduces the system behavior within reasonable bounds to satisfy the objectives of the analysis. Various approaches to validation include expert intuition, theoretical results or analysis and real system measurements (Hillston, 2003). During validation, the modeller is required to consider assumptions made, input values and their statistical distributions, output values and their distributions.

Model calibration and validation algorithms available in SWAT-CUP include Sequential Uncertainty Fitting (SUFI2), Parameter Solution (Parasol), Generalized Likelihood Uncertainty Estimation (GLUE) and Markov Chain Monte Carlo (MCMC). The conceptual basis of the algorithms is described in (Abbaspour, 2015b), SWAT-CUP: SWAT Calibration and Uncertainty Programs-A User Manual. SWAT-CUP has been widely applied in SWAT studies in various parts of the world (Arnold *et al.,* 2012).

SWAT-Check

During calibration and validation, the model may contain inappropriate parameter adjustments and data errors. SWAT-Check (White, Harmel, Arnold, and Williams, 2014) is used for automated checking of errors and detecting common model application problems. It is a stand-alone computer program that can examine 56 model output and summaries and signal the modeller when unusual values are encountered (Arnold *et al.,* 2012).

2.2   Sediment Yield

The amount of soil loss delivered at an outlet of a catchment is called sediment yield. The ratio of the sediment yield to gross soil loss is called sediment delivery ratio, SDR (Borah *et al.,* 2008). This is illustrated in the following equation:

$$SDR = \frac{SY}{GE} \tag{2.15}$$

Where,

SDR = sediment delivery ratio (no units),

SY = sediment yield (mass per unit area per unit time),

GE = gross erosion (mass per unit area per unit time).

An empirical form of the equation is expressed by Ward and Trimble (2003) as:

$$SDR = \left[\left(\frac{q_{peak}}{R_{peak}} \right) \left(0.78285 + 0.21716 \frac{Q}{R} \right) \right]^{0.56} \tag{2.16}$$

Where,

q_{peak} = peak runoff rate (mm per unit time),

R_{peak} = peak rainfall rate (mm per unit time),

Q = total runoff (mm),

R = total rainfall (mm),

0.56 = constant

CHAPTER THREE

MATERIALS AND METHODS

3.1 Study Area

Figure 3.1. A map showing the area of study.
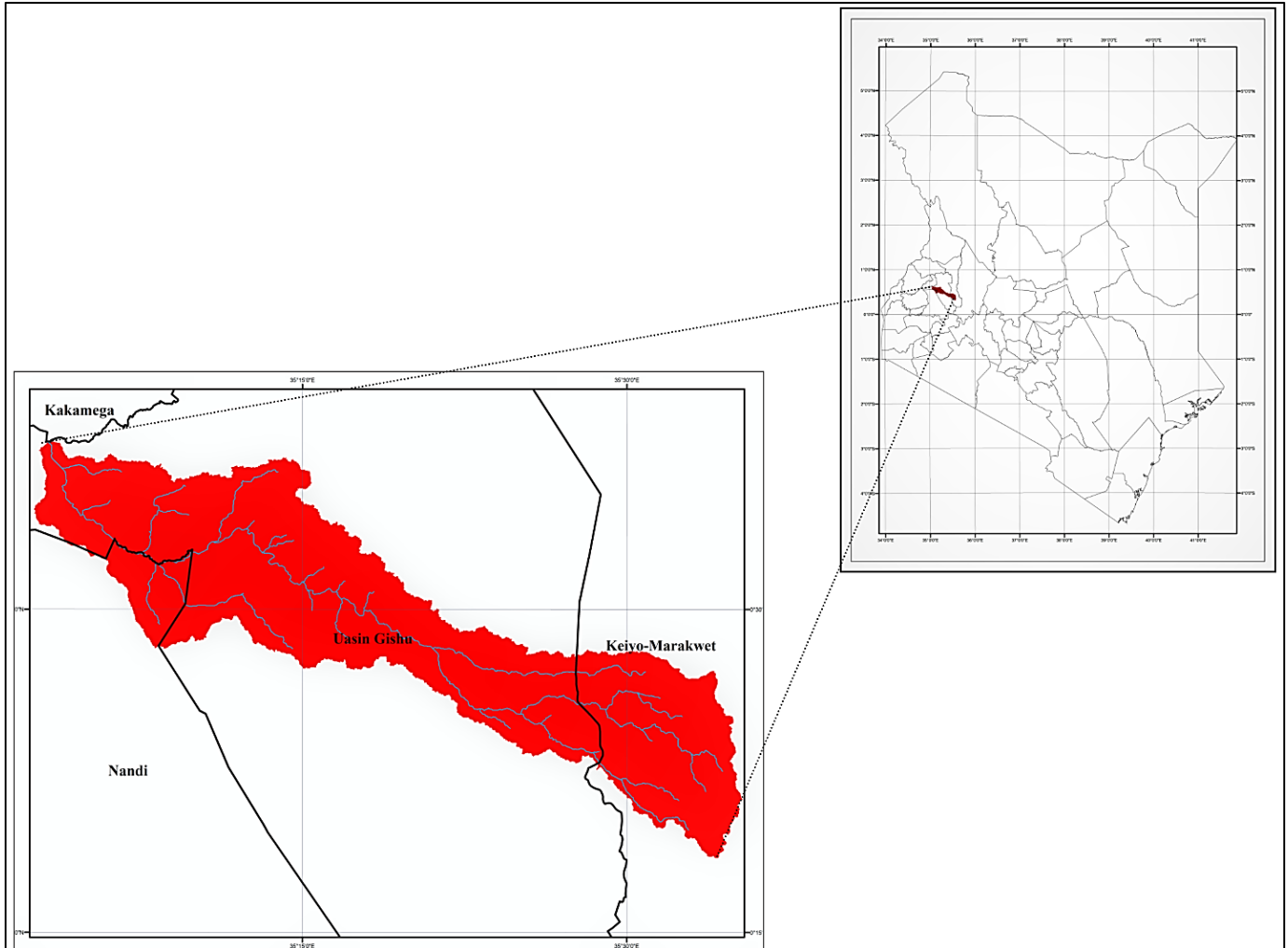
The study was conducted in Sosiani catchment in the upper region of the larger Nzoia catchment. Sosiani is a trans-boundary river flowing across the boundaries of three counties: Keiyo Marakwet, Uasin Gishu and Nandi counties in Kenya. The catchment lies between longitudes 35° 2' 37.274" E and 35° 35' 16.354" E, and latitudes 0° 18' 24.039" N and 0° 37' 42.923" N (figure 3.1). Sosiani catchment has an area of 657.6 km^2 and a perimeter of

272.934 km. The altitude of the catchment ranges between 1800 metres and 2755 metres above sea level. A large part of the catchment has a slope that ranges between 0.0 % and 6.5 % percent rise. The catchment receives high annual rainfall ranging between 1200 mm and 1600 mm and contributes about 30 % of the flow in River Nzoia (Oruta, 2016). The catchment covers 48 sub-locations and 14 towns, including Eldoret Town, the headquarters of Uasin Gishu County (figure 3.2)

Figure 3.2. A map showing Sosiani River network, major towns and sub-locations.
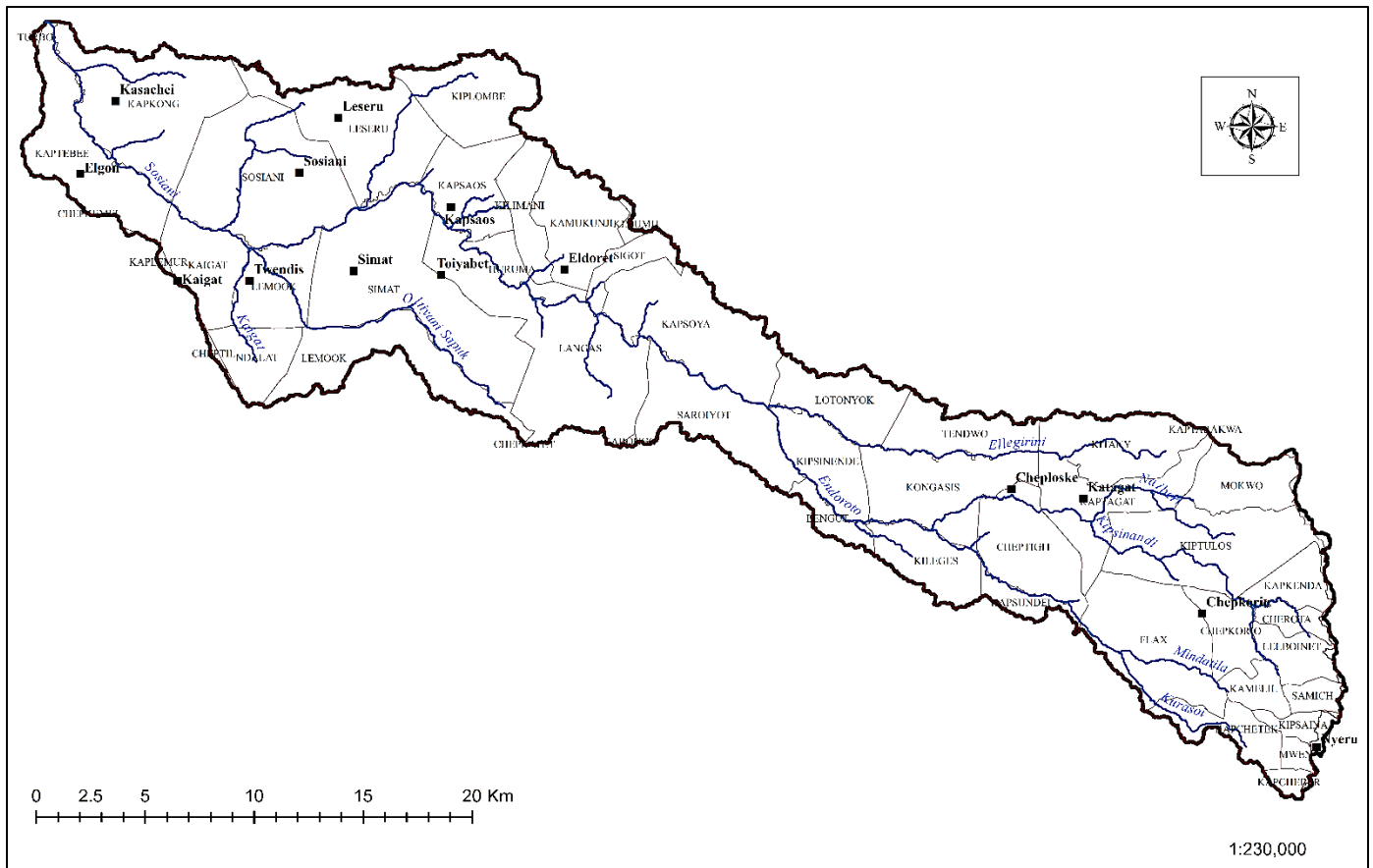
3.2 Data Collection, Preparation and Exploratory Analysis

Data collection involved acquiring datasets needed from relevant sources and authorities. The data used in the study was categorized into four classes: geographic information systems (GIS) data, flow data, sediment data and weather data. GIS data included elevation data, land cover data and soil data. The digital elevation model data [Shuttle Radar Topography Mission (SRTM GL1) Global 30m)] was obtained from OpenTopography website (NSF OpenTopography Facility, 2013).

Soil data was obtained from FAO Harmonized World Soil Database (HWSD) version 1.2 and the HWSD raster file (FAO/IIASA/ISRIC/ISS-CAS/JRC, 2009). Land cover data was obtained from United States Geological Society (USGS) Earth Explorer (USGS, 2017), as three-band (2,3,4) images from Landsat 8 OLI-TIRS [OLI (Operational Land Imager) and TIRS (Thermal Infrared Sensor)]. Daily weather data (precipitation, wind, relative humidity, and solar) from 1st January 1984 to 31st July 2014 was obtained global weather data SWAT prepared by United States National Center for Environmental Prediction (NCEP) Climate Forecast System Reanalysis (CFSR) (NCEP, 2017). Observed river flow data for the river gauging station (Sosiani 1CB05) at the outlet of the catchment was obtained from Water Resources Authority (WRA). The length of the dataset was from 1984 to 2014. Efforts to acquire sediment data from relevant authorities were not fruitful.

Data preparation and exploratory analysis involved checking for integrity and consistency (graphical plots and basic statistics) of acquired datasets. It also involved formatting of the datasets for the modelling exercise according to standard ArcSWAT input-output formats (Arnold *et al.,* 2011).

Digital Model Data (DEM)

The digital elevation model data was downloaded with a spatial reference GCS_WGS_1984. The first step was to re-project the digital elevation model to Arc_1960_UTM_Zone_36N using the following syntax in ArcGIS ArcMap interface: geoprocessing Tools; Arc Toolbox; Data Management Tools; Projections and Transformations; Raster; Project raster. The area of the digital elevation model representing the study area was extracted based on the shape file of the catchment using the following syntax: geoprocessing Tools; Arc Toolbox; Spatial Analyst Tools; Extraction; Extract by mask. Hillshade was developed by using: geoprocessing Tools; Arc Toolbox; Spatial Analyst Tools; Surface; Hillshade. The result was used together with the digital elevation model to produce an elevation map (figure 3.4).

Figure 3.4. Elevation map of Sosiani catchment.
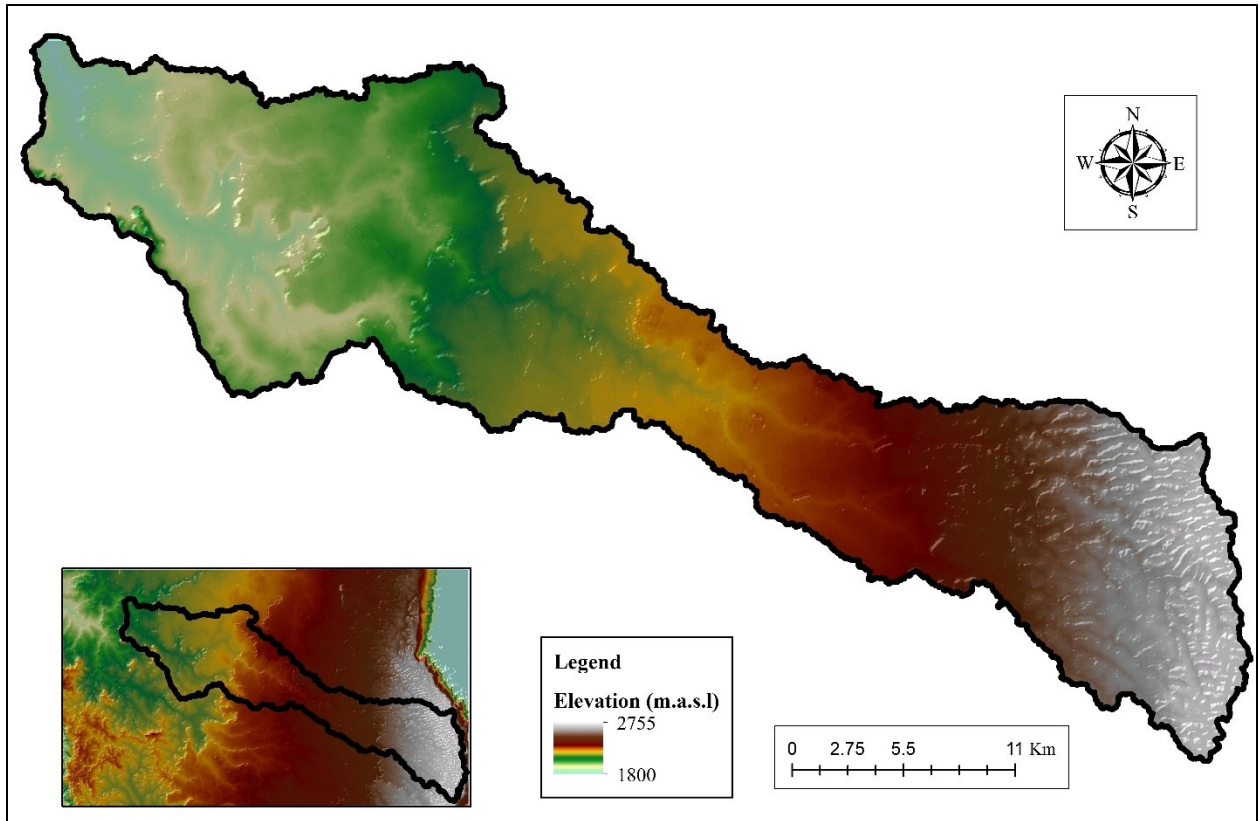
The slope was estimated using the syntax: geoprocessing Tools; Arc Toolbox; Spatial Analyst Tools; Surface; Slope. Aspect map was developed using the syntax: geoprocessing Tools; Arc Toolbox; Spatial Analyst Tools; Surface; Aspect.

Figure 3.5. Slope and Aspect map of Sosiani Catchment
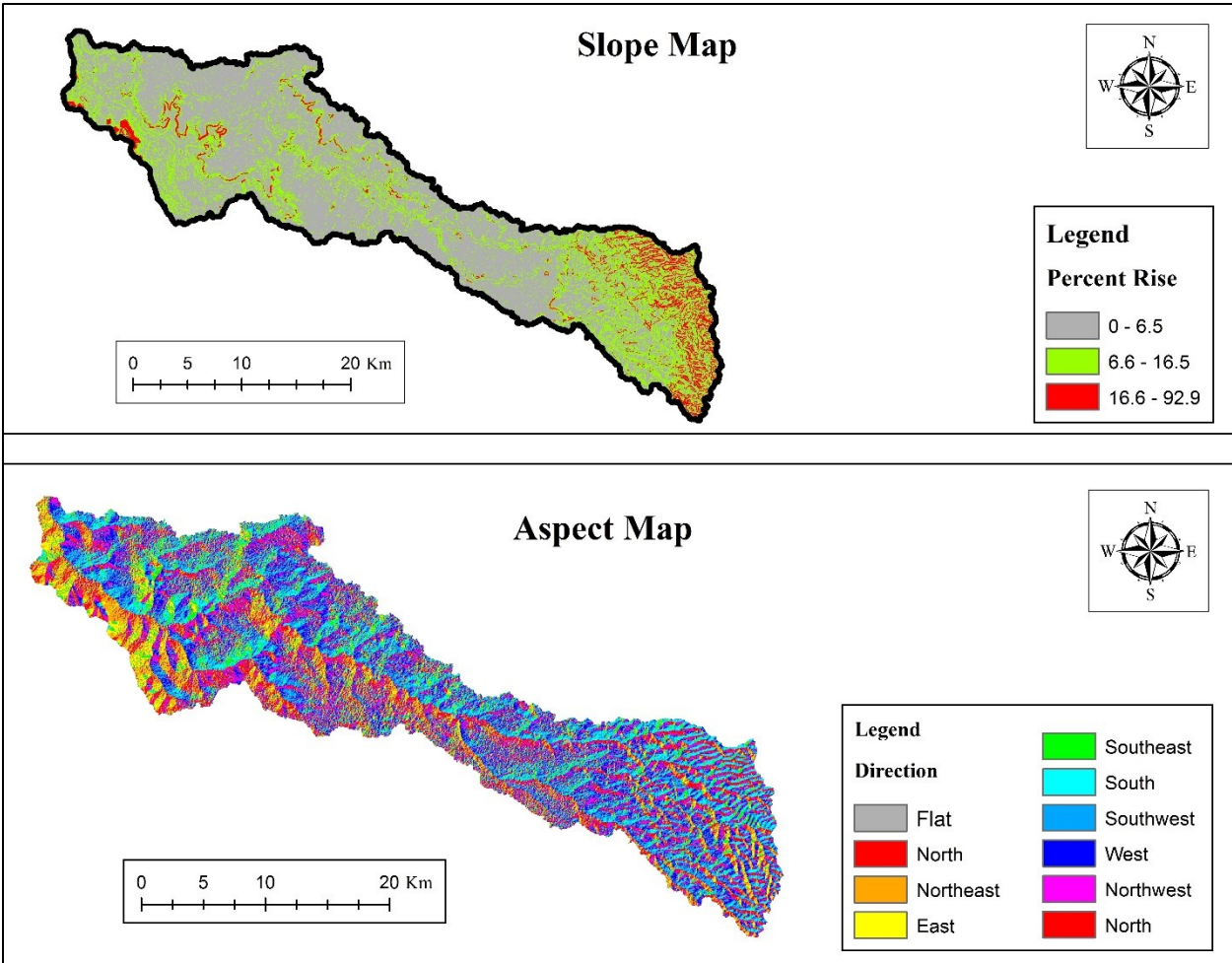
The digital elevation model was processed using Arc Hydro Tools to produce a river network shape file that was used to guide ArcSWAT to delineate the watershed

Land Cover Data

Land cover data included two Landsat 8 images acquired on 16th January 2014, 0750h [image id LC81700602014LGN00; minimum latitude -1.05414, minimum longitude 33.2987, maximum latitude 1.04709, maximum longitude 35.3406; 10% cloud cover] and 25th January 2014, 0745h [image id LC8169060202014025LGN00; minimum latitude -1.05422, minimum longitude 34.8264, maximum latitude 1.04696, maximum longitude 36.8675; 0% cloud cover]. The images were downloaded and pre-processed (atmospheric correction and dark object subtraction) using semi-automatic classification Tool in Quantum GIS (QGIS Development Team,

2017). Mosaicking was done using Seamless Mosaicking Tool and classified using ISODATA classification Tool in Environment for Visualizing Images (ENVI) version 5.1 (Exelis, 2013).

Figure 3.6 Land cover images.
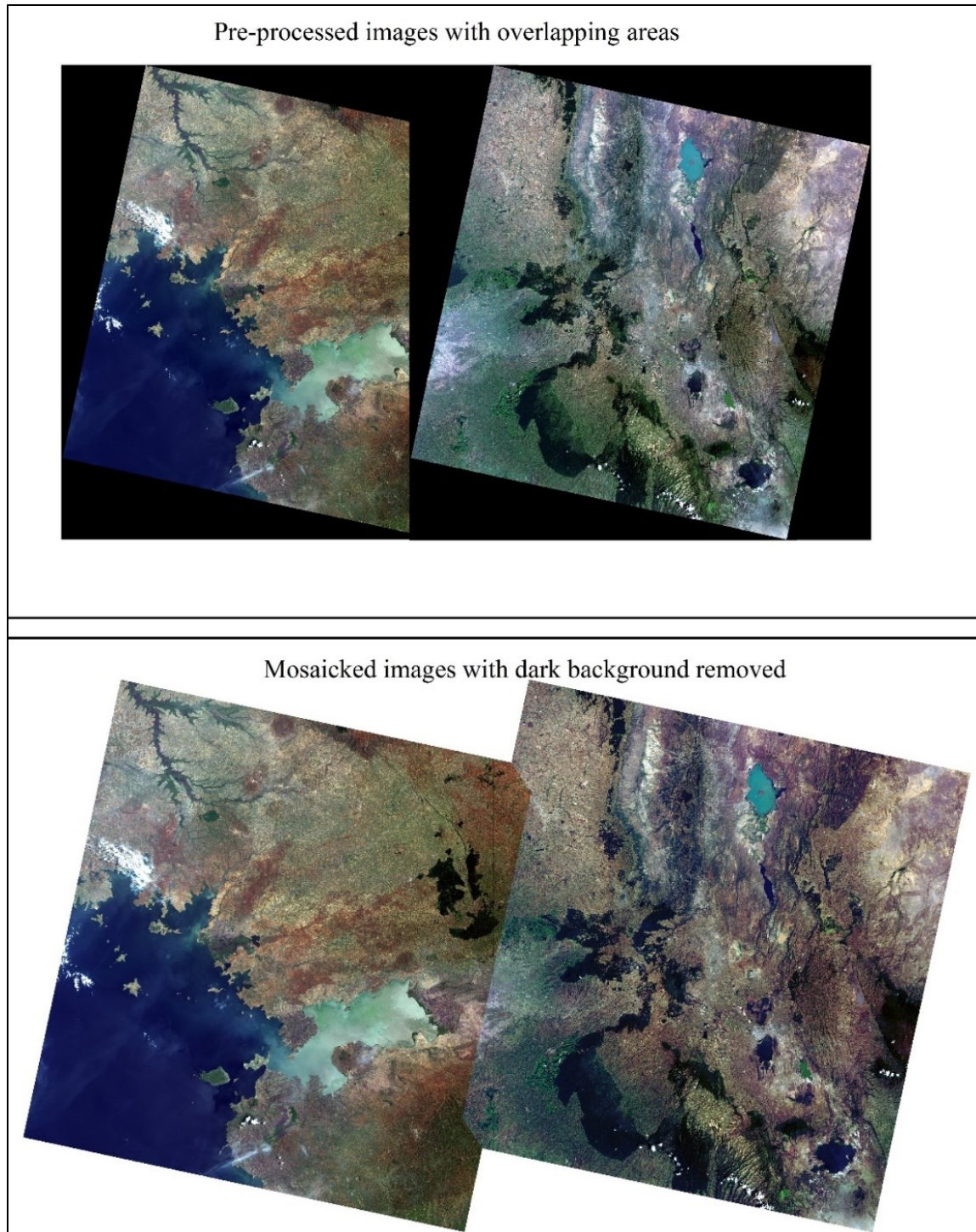
The portion of the mosaic image that fell under Sosiani catchment was clipped using Feature Extraction Tool in ENVI 5.1 based on Sosiani catchment shapefile as the mask. The image clip was classified into four land cover categories: agriculture, forest, urban and rangeland.

Figure 3.6. Major land use/land cover classes in Sosiani Catchment.
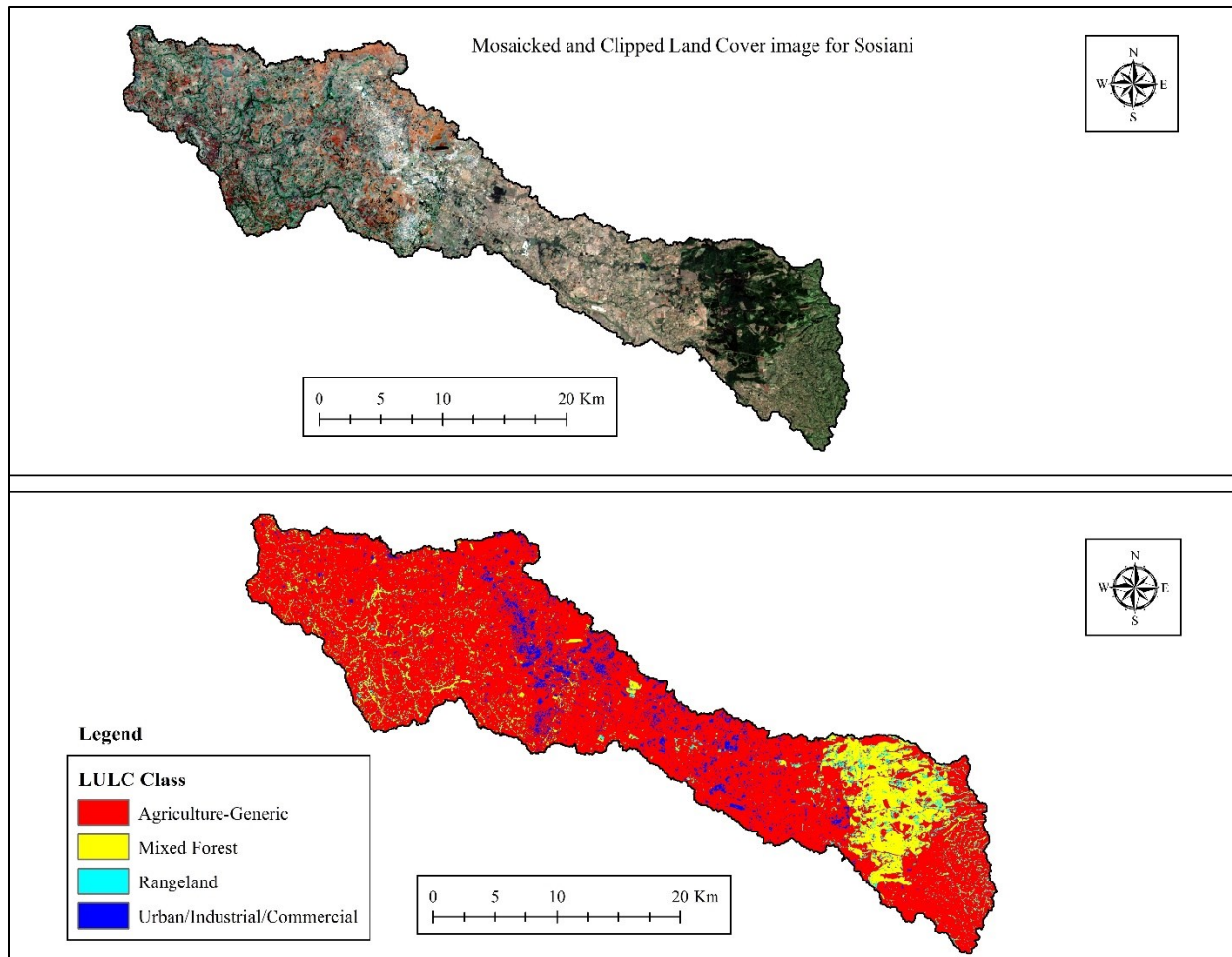
A land use look-up table was created using Notepad. The table was used in land use/soils/slope definition. The structure of the land use look-table is as shown

Table 3.1. Look-up table for Sosiani land use.

"Value", "Landuse"
1, UCOM
2, FRST
3, RNGE
4, AGRL

Where "value" is the number of map category and "landuse" is the corresponding SWAT landuse or urban code.

Soil Data

The harmonized world soil database was loaded into ArcGIS using the following syntax:

"Open *ArcCatalog*. Click *Customize* tab on the tool bar. Click *Customize*. Click *Commands*. Click *ArcCatalog*. From the menu box that opens, drag and drop *Add OLE DB connection* on the tool bar. Double click on the *Add OLE DB connection icon* you've just added on the tool bar. From the menu box that opens, click once on *Microsoft je4.0 OLE DB provider*. Click *next*. From the dialog box that opens, *browse to the location* where you stored HWSD. Click once on the HWSD. Click *Add*. On the *Catalog Tree*, right-click on *database connections*. Choose *Refresh*. Click on *OLE DB connection (2).odc*. You will see the *contents* loaded in the view pane. Go to *ArcMap*. Add *hwsd.bil*. Click on *Search icon* on the tool bar. In the *search dialog box*, type *raster table*. From the options, double-click on *Build Raster Attribute Table*. In the *Input Raster* dialog menu, choose *hwsd.bil*. Click *OK*. After the program completes building the attribute table, right-click on *hwsd.bil*. Choose *Joins and Relates*, then choose *Join*. In the *first* dialog menu, choose *Value*. In the *second* dialog menu, *browse* to *Database Connections* and double-click on *OLE DB connection (2).odc.*, choose *HWSD_DATA*, then click *Add*. In the *third* dialog menu, choose *MU_GLOBAL*, then click *OK*. To see the attribute table, right-click on *hwsd.bil* and choose *Open Attribute Table*."

The soil for Sosiani was extracted using Spatial Analyst, Extract by Mask Tool the hwsd.bil as the Input Raster and Sosiani catchment shapefile as the mask

Figure 3.8. Soil Classes in Sosiani catchment.
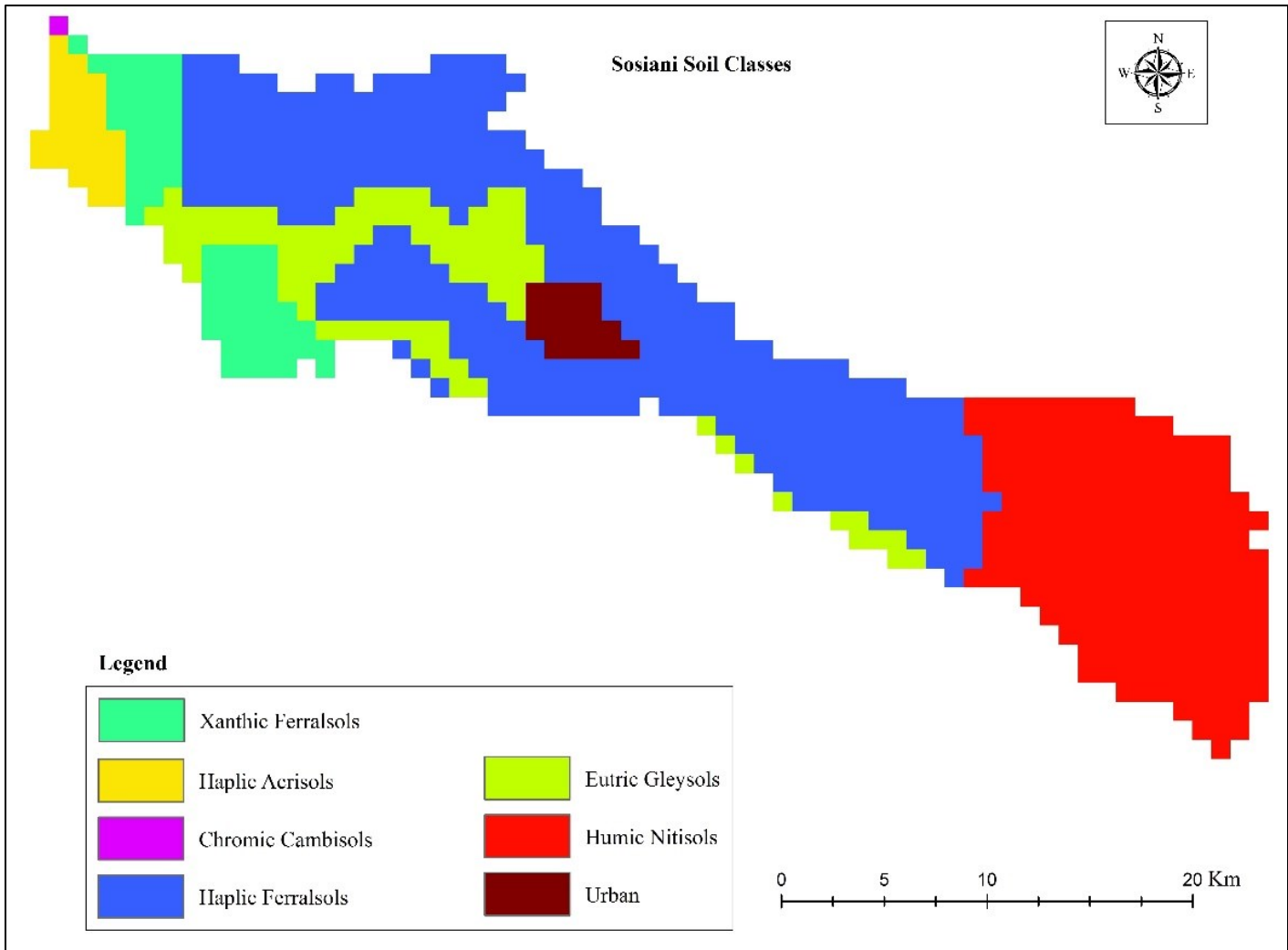
The analysis showed that there are seven soil classes in Sosiani catchment. The classes include Xanthic Ferralsols, Haplic Acrisols, Chromic Cambisols, Haplic Ferralsols, Eutric Gleysols, Humic Nitisols and Urban. The following table is a summary of the major characteristics of the soil classes.

Table 3.2. Selected Sosiani top-soil properties.

Class	Drainage	Texture	USDA Texture	Percent Gravel	Percent Sand	Percent Silt	Percent Clay	Percent Organic Carbon	Bulk Density
Humic Nitisols	Moderately well	Fine	Clay (light)	0	19	31	50	2.2	1.33
Haplic Acrisols	Moderately well	Medium	Clay loam	21	42	25	33	1.48	1.22
Chromic Cambisols	Moderately well	Medium	Sandy clay loam	16	55	15	30	1.15	1.3
Haplic Ferralsols	Moderately well	Fine	Clay (heavy)	0	26	10	64	1.17	1.2
Eutric Gleysols	Very poor	Fine	Clay (heavy)	0	15	25	60	1.95	1.13
Xanthic Ferralsols	Moderately well	Fine	Clay (heavy)	0	30	10	60	1.41	1.2
Urban	None	None	None	None	None	None	None	None	None

Table 3.3. Selected Sosiani Sub-soil properties.

Class	Drainage	Texture	USDA Texture	Percent Gravel	Percent Sand	Percent Silt	Percent Clay	Percent Organic Carbon	Bulk Density
Humic Nitisols	Moderately well	Fine	Clay (heavy)	0.0	12.0	20.0	68.0	1.0	1.4
Haplic Acrisols	Moderately well	Medium	Clay (light)	1.0	35.0	25.0	40.0	0.7	1.3
Chromic Cambisols	Moderately well	Medium	Sandy clay	28	50.0	10.0	40.0	0.8	1.4
Haplic Ferralsols	Moderately well	Fine	Clay (light)	0.0	38.0	8.0	54.0	1.0	1.3
Eutric Gleysols	Very poor	Fine	Clay (light)	0.0	39.0	7.0	54.0	0.6	1.3
Xanthic Ferralsols	Moderately well	Fine	Clay (light)	0.0	32.0	10.0	58.0	0.6	1.2
Urban	None	None	None	None	None	None	None	None	None

K_{USLE} factor was calculated based on percent sand, percent silt, percent clay and percent organic carbon; using the following equation as described in SWAT theoretical documentation version 2009 (Neitsch *et al., 2*011b):

$$K_{USLE} = f_{csand} \times f_{cl\text{-}si} \times f_{orgc} \times f_{hisand} \qquad (3.1)$$

Where,

$$f_{csand} = \left[0.2 + 0.3 \times \exp\left(-0.256 \times m_s \times \left(1 - \frac{m_{silt}}{100}\right)\right)\right] \qquad (3.2)$$

$$f_{cl\text{-}si} = \left(\frac{m_{silt}}{m_c + m_{silt}}\right)^{0.3} \qquad (3.3)$$

$$f_{orgc} = \left[1 - \frac{0.25 \times orgC}{orgC + \exp(3.72 - 2.95 \times orgC)}\right] \qquad (3.4)$$

$$f_{hisand} = \left[1 - \frac{0.7 \times \left(1 - \frac{m_s}{100}\right)}{\left(1 - \frac{m_s}{100}\right) + \exp\left(-5.51 + 22.9 \times \left(1 - \frac{m_s}{100}\right)\right)}\right] \qquad (3.5)$$

With m_s = percent sand; m_{silt} = percent silt; m_c = percent clay and orgC = percent carbon of the layer.

f_{csand} is a factor that gives low soil erodibility for soils with high coarse-sand contents and high values for soils with little sand.

$f_{cl\text{-}si}$ is a factor that gives low soil erodibility for soils with high clay to silt ratios.

f_{orgc} is a factor that reduces soil erodibility for soils with high organic carbon content.

f_{hisand} is a factor that reduces soil erodibility for soils with extremely high sand contents.

Table 3.4. Computed USLE-K factors for Sosiani Soils.

| Class | Computed Values | | | | |
| | Top-Soil | | | | |
	f_{csand}	f_{cl-si}	f_{orgc}	f_{hisand}	K_{USLE}
Humic Nitisols	0.2105	0.7497	0.7569	0.9844	0.1195
Haplic Acrisols	0.2001	0.7769	0.8154	0.9813	0.1267
Chromic Cambisols	0.2000	0.7192	0.8867	0.9766	0.1272
Haplic Ferralsols	0.2008	0.5486	0.8820	0.9837	0.0972
Eutric Gleysols	0.2168	0.6927	0.7657	0.9847	0.1150
Xanthic Ferralsols	0.2003	0.5578	0.8284	0.9834	0.0926
Urban	None	None	None	None	None

Saturated hydraulic conductivity and available water capacity of the of the soil layers were calculated using SPAW model (Saxton, 2007) based on Saxton and Rawls (2006). On the SPAW interface, layer-specific values for sand, clay, gravel and organic carbon contents were input into the model. The output consisted among other values, the values for saturated hydraulic conductivity and available water capacity of the specific soil class layers.

Table 3.5. Saturated hydraulic conductivity of Sosiani soil layers.

| Class | Computed values for saturated hydraulic conductivity, K, (mm/hr.) and available water capacity, AWC, (mm/mm). | | | |
| | Top-Soil | | Sub-Soil | |
	K	AWC	K	AWC
Humic Nitisols	1.58	0.13	1.62	0.13
Haplic Acrisols	2.61	0.10	1.42	0.13
Chromic Cambisols	3.94	0.09	0.70	0.08
Haplic Ferralsols	0.20	0.12	0.11	0.12
Eutric Gleysols	0.97	0.11	0.09	0.12
Xanthic Ferralsols	0.09	0.12	0.10	0.12
Urban	None	None	None	None

The soil classes were classified into hydrologic soil groups according to Natural Resources Conservation Service (2007) classification. According to the classification, generally:

Group A soils: contain less than 10 percent clay and more than 90 percent sand or gravel. They have gravel or sand textures. Saturated hydraulic conductivity of all soil layers is more than 144mm/hr. The depth to any water impermeable layer is greater than 500 mm.

Group B soils: contain 10 percent to 20 percent clay and 50 percent to 90 percent sand. They have loamy sand or sandy loam textures. Saturated hydraulic conductivity ranges between 36mm/hr. and 144mm/hr. The depth to any water impermeable layer is greater than 500 mm.

Group C soils: contain 20 percent to 40 percent clay and 50 percent or less sand. They have loam, silt loam, sandy clay loam, clay loam, and silty clay loam textures. Saturated hydraulic conductivity is between 3.6mm/hr. and 36mm/hr. The depth to any water impermeable layer is greater than 500 mm.

Group D soils: contain more than 40 percent clay, less than 50 percent sand. They have clayey textures. Saturated hydraulic conductivity is equal to or less than 3.6mm/hr. The depth to any water impermeable layer is 500mm.

The soil database for Sosiani lacked information about depth to water impermeable layer. The hydrologic soil groups were assigned based on saturated hydraulic conductivity, percent sand and percent clay.

Table 3.6. Hydrologic Soil Groups in Sosiani catchment.

Soil Class	Hydrologic Soil Group [Considering topsoil only]
Humic Nitisols	D
Haplic Acrisols	D
Chromic Cambisols	C
Haplic Ferralsols	D
Eutric Gleysols	D
Xanthic Ferralsols	D
Urban	None

This information was used to prepare a user soil database in Microsoft excel with a structure similar to ArcSWAT default user soil database. The required parameters included hydrologic soil group (A, B, C or D), maximum rooting depth of soil profile (mm), depth from soil surface to bottom of the soil layer (mm), moist bulk density (Mg/m3 or gm/cm3), available water capacity of the soil (mm of water/mm of soil), saturated hydraulic conductivity (mm/hr.); organic carbon content, clay content, sand content, silt content and rock fragment content, all as percent of soil weight; moist soil albedo and USLE soil erodibility factor for the topsoil. The moist soil albedo was set to 0.13, according to Gijsman, Thornton, and Hoogenboom (2007). The rock fragment content was taken as the gravel content. The soil the soil database was appended to the *usersoil* table in the *SWAT2012.mdb* database found in the databases sub-folder in the SWAT installation folder.

A soil look-up table was created in Notepad. The look-up table was used to link the soil raster file and the SWAT soil usersoil, during landuse/soil/slope definition. The structure of the look-up table is as shown:

Table 3.7. Look-up table for Sosiani Soil

"Value", "Name"
17494, CMx
17678, FRh
17707, Gle
17709, FRr
17713, Ur
17318, Ntu
17438, Ach
17790, Ntu

Weather Data

Weather data included Climate Forecast System Reanalysis (CFSR) world monthly weather database and daily weather time series data for 8 CFSR weather stations within the vicinity of the study area. The CFSR weather database was imported into the ArcSWAT weather database using the import tool in the Microsoft Access interface.

Rainfall data

A total of 8 rainfall datasets from the 8 weather stations were downloaded.

Table 3.8. CFSR weather stations in the vicinity of Sosiani catchment.

Station Code	Longitude	Latitude
2350	35.0000	0.156113997
2353	35.3125	0.156113997
5350	35.0000	0.468342990
5353	35.3125	0.468342990
5356	35.6250	0.468342990
8350	35.0000	0.780571997
8353	35.3125	0.780571997
8356	35.6250	0.780571997

Figure 3.9. Map of CFSR weather stations in the vicinity of Sosiani catchment.
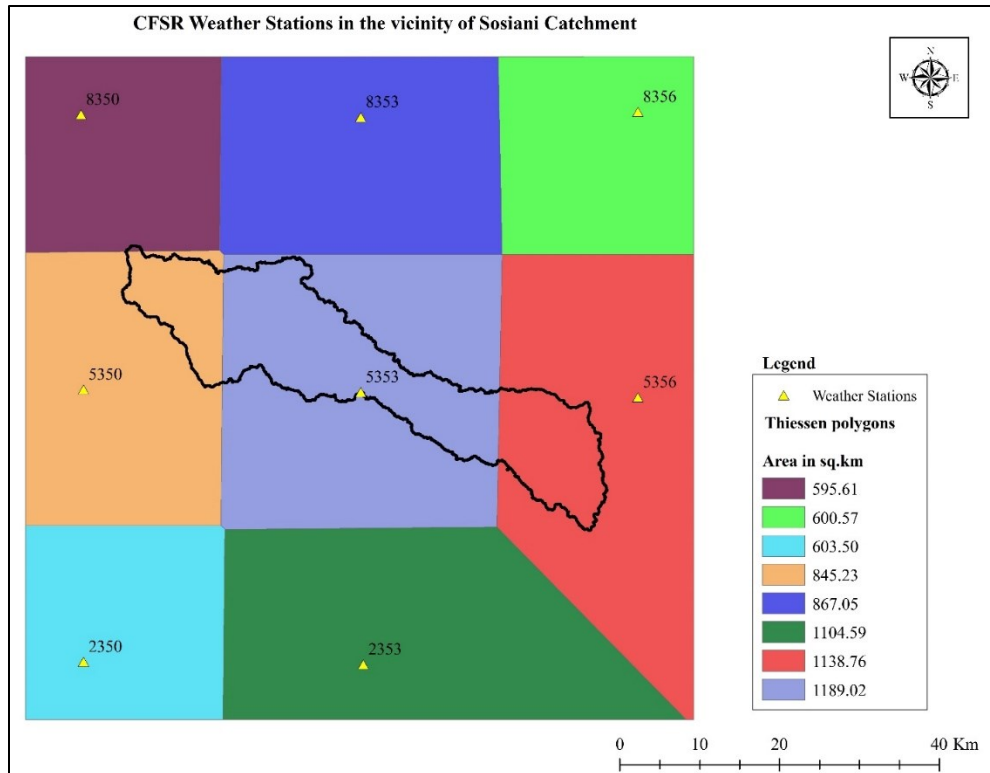
From the list of the 8 weather stations, 3 weather stations were selected as shown in the following figure.

Figure 3.10. Selected weather stations and thiessen areas.
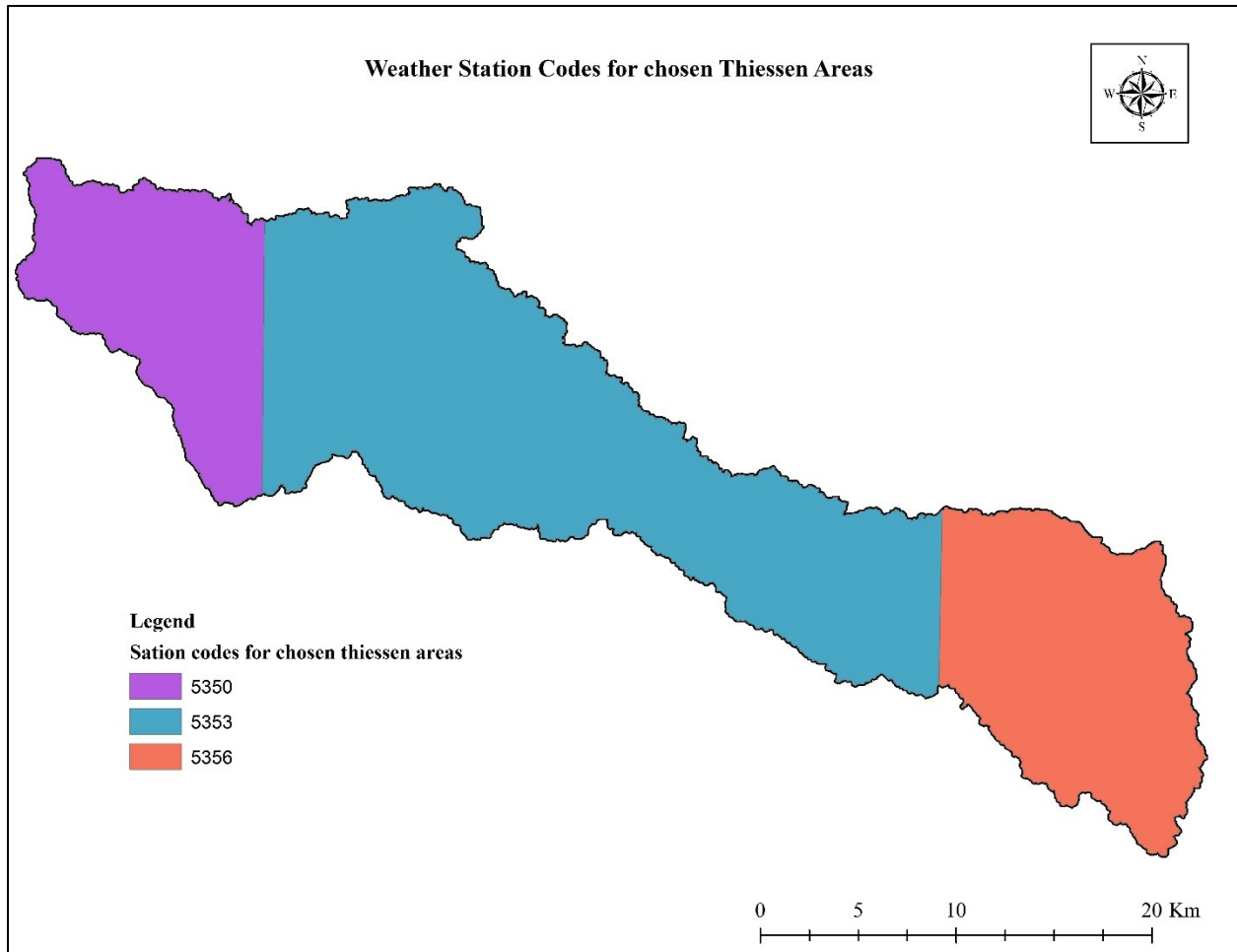
The average areal rainfall for Sosiani catchment was calculated using thiessen polygon method (Schumann, 1998):

$$\bar{P} = \sum_i^n P_i \frac{A_i}{A} \qquad (3.6)$$

Where:

$\bar{P}$ = average areal rainfall (mm)

P_i = rainfall at a station i (mm)

A_i = polygon area for a particular station i (km^2)

A = sum of polygon areas (km^2).

Table 3.9. Annual rainfall for rain stations in the vicinity of Sosiani catchment.

Year	Annual Rainfall (mm)		
	5356	5350	5353
1984	424.50	1149.34	1305.29
1985	744.91	1970.57	1896.49
1986	1046.64	1543.49	1816.23
1987	548.26	1533.58	1273.11
1988	929.07	2178.61	2139.91
1989	435.35	1091.81	1218.14
1990	613.50	1640.17	1689.42
1991	661.12	1508.58	1656.92
1992	615.07	1314.28	1494.03
1993	367.79	1046.51	1244.19
1994	887.41	1763.95	1961.72
1995	541.72	1336.72	1487.02
1996	498.64	1234.50	1272.74
1997	643.16	1446.86	1392.39
1998	986.34	1541.90	1877.25
1999	203.99	1289.29	1247.21
2000	595.85	1401.71	1666.64
2001	541.73	1516.55	1602.83
2002	521.30	1358.37	1285.13
2003	622.51	1805.72	1673.54
2004	439.97	1331.28	1278.94
2005	863.72	1774.03	1828.55
2006	654.61	1801.38	1667.25
2007	856.82	1998.36	1818.42

2008	637.88	1815.78	1740.47
2009	210.44	836.91	802.858
2010	1962.00	2965.38	2964.25
2011	1767.68	1452.24	3118.56
2012	1688.52	1183.45	2727.24
2013	2328.33	1369.24	3189.65
Average	**794.63**	**1540.02**	**1744.55**

Table 3.10. Thiessen polygon areas for selected stations

Station	Area of thiessen polygon (km^2)
5353	367.07
5356	163.20
5350	127.33

Table 3.11. Computation for annual average areal rainfall.

A= 657.6 km^2				
Station	**A_i (km^2)**	**$A_i \div A$**	**Annual P_i (mm)**	**P_i $(A_i \div A)$ (mm)**
5353	367.07	0.56	1744.55	976.95
5356	163.20	0.25	794.63	243.66
5350	127.33	0.19	1540.02	292.60
			Sum	**1513.21**

Basic exploratory data analysis was done using MINITAB statistical software (MINITAB Inc., 2004). The following figures show basic statitsics summary and probabillity plots for the rainfall

Figure 3.11. Basic statistics graphical summary for Sosiani Rainfall.

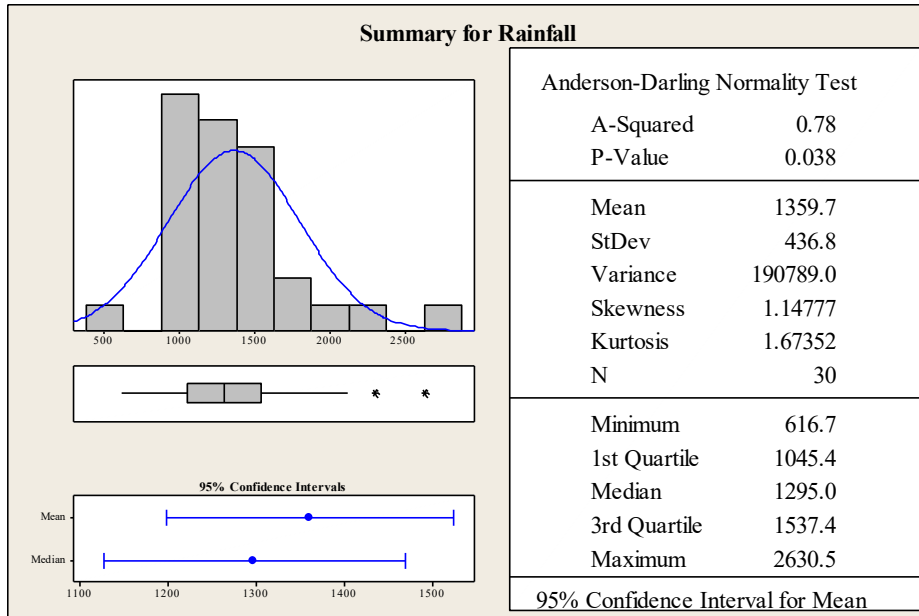Figure 3.12. Gamma distribution probalility plot for Sosiani rainfall.
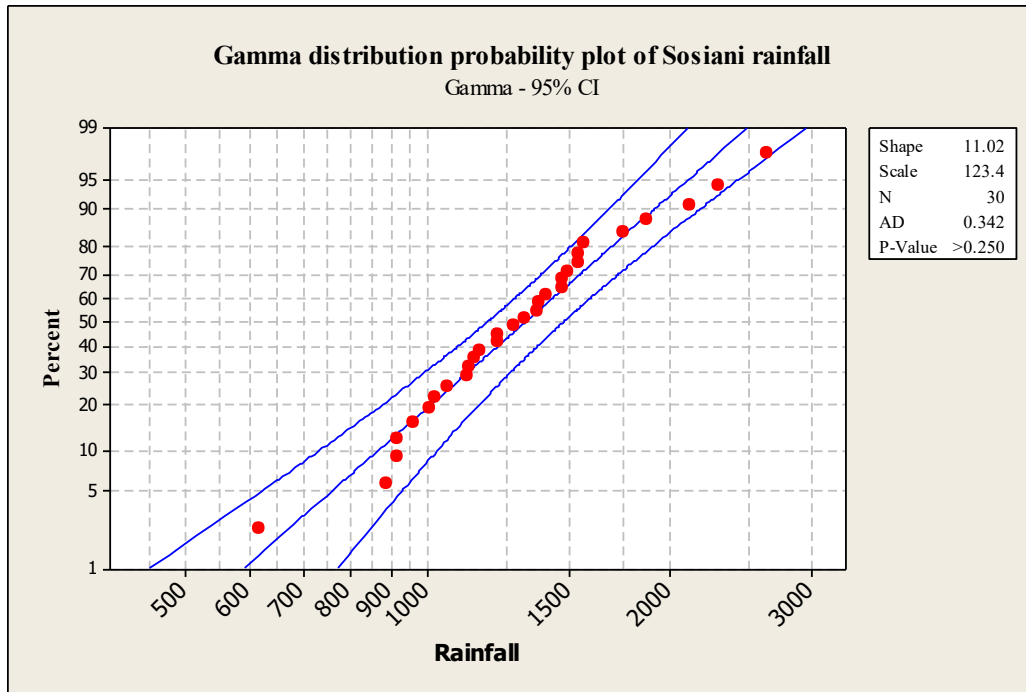
Figure 3.13. Normal distribution probability plot of Sosiani rainfall.

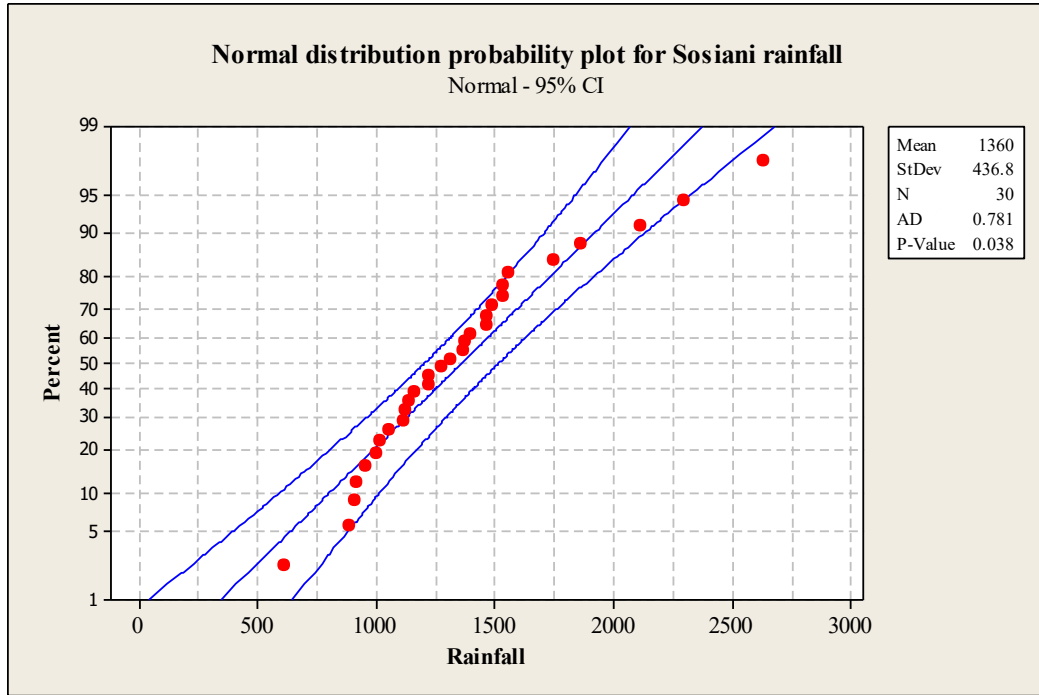**Normal distribution probability plot for Sosiani rainfall**
Normal - 95% CI

Mean	1360
StDev	436.8
N	30
AD	0.781
P-Value	0.038

Figure 3.14. Box-plot for Sosiani rainfall

Boxplot of Sosiani Rainfall
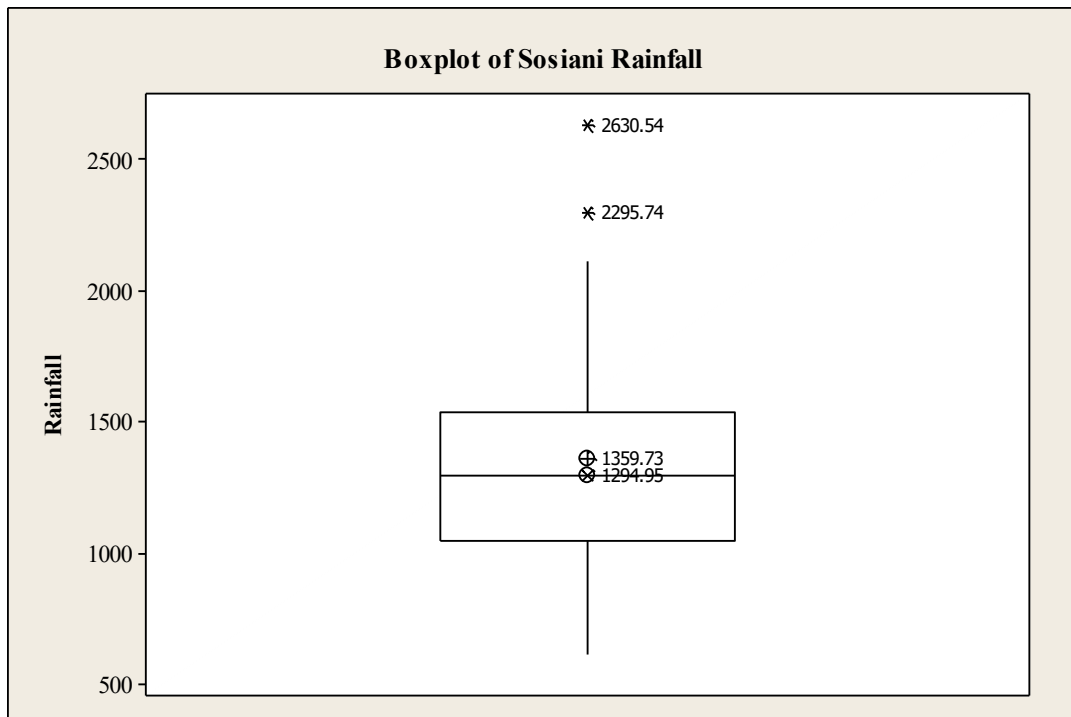
Figure 3.15. Sosiani annual rainfall time series.
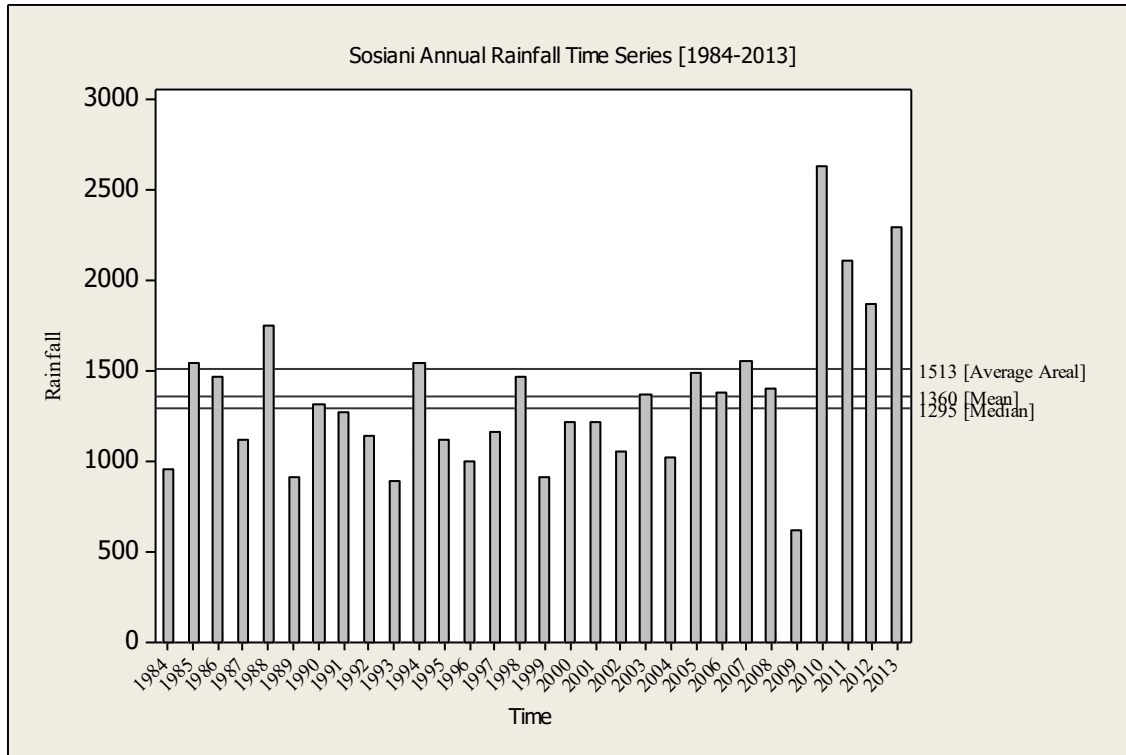
Sosiani rainfall exhibits gamma distribution. The years 2010,2011,2012,2013 had abnormally high rainfall.

The rainfall parameters required by ArcSWAT weather generator were calculated using the program pcpSTAT .exe (Stefan, 2003). The program is used to estimate specific statistical parameters of daily precipitation data. The parameters are described in the following table:

Table 3.12. Statistical precipitation parameters used in SWAT

Parameter	Description
PCPMM(mon)	Average or mean total monthly precipitation
PCPSTD(mon)	Standard deviation for daily precipitation in month
PCPSKW(mon)	Skew coefficient for daily precipitation in month
PR_W1(mon)	Proability of a wet day following a dry day
PR_W2(mon)	Probability of wet day following a wet day
PCPD(mon)	Average number of days of precipitation in month

Table 3.13. Statitiscal rainfall parameters for station 5350 for the period 1984 – 2012.

Month	PCPMM	PCPSTD	PCPSKW	PR_W1	PR_W2	PCPD
Jan	18.58	2.6108	7.0853	0.1442	0.6525	9.72
Feb	26.45	3.8224	6.1943	0.1318	0.6654	9.17
Mar	53.96	5.9333	6.6194	0.1873	0.738	13.69
Apr	245.86	13.7376	2.7954	0.5	0.8874	25.72
May	230.92	10.8081	3.6124	0.4384	0.9274	28.48
Jun	248.48	9.8895	2.2691	0.4255	0.9465	28.38
Jul	211.05	8.4795	2.6602	0.6053	0.9408	29.69
Aug	226.4	9.0249	2.2835	0.6222	0.9333	29.45
Sep	95.9	6.2801	4.2671	0.5035	0.8669	25.14
Oct	102.05	6.3802	4.2463	0.5227	0.8761	26.45
Nov	59.81	5.5309	6.4648	0.2758	0.7652	17.62
Dec	26.49	2.9401	5.0826	0.1681	0.6677	11.31

Table 3.14. Statistical rainfall parameters for station 5353 for the period 1984 – 2012.

Month	PCPMM	PCPSTD	PCPSKW	PR_W1	PR_W2	PCPD
Jan	17.11	2.573	7.0842	0.1161	0.6314	8.14
Feb	26.14	3.8728	5.8632	0.11	0.6303	7.28
Mar	49.15	5.2812	6.238	0.1727	0.6968	11.83
Apr	248.9	13.0497	2.6125	0.4335	0.8637	24.03
May	233.75	9.8766	2.9015	0.3942	0.8963	26.28
Jun	277.31	10.1348	2.1445	0.4444	0.9424	28.14
Jul	278.83	8.9232	2.1294	0.7368	0.9523	30.34
Aug	267.48	9.6048	1.9571	0.5455	0.922	28.72
Sep	106.78	6.6328	2.9765	0.3604	0.8395	22.34
Oct	110.03	6.3512	3.5879	0.4717	0.8662	25.52
Nov	59.85	4.7897	4.1217	0.2595	0.764	17.24
Dec	19.66	2.3996	5.6963	0.1506	0.6424	9.93

Table 3.15. Statistical rainfall parameters for station 5356 for the period 1984 – 2012.

Month	PCPMM	PCPSTD	PCPSKW	PR_W1	PR_W2	PCPD
Jan	4.19	0.9794	12.2985	0.0456	0.5287	3
Feb	9.16	2.3709	11.9349	0.0481	0.5652	3.17
Mar	19.14	3.3222	9.7751	0.1004	0.5879	6.28
Apr	142.2	10.421	3.5332	0.3136	0.7838	18.34
May	95.65	6.712	4.5195	0.2447	0.7881	17.9
Jun	122.44	7.1142	3.5785	0.3383	0.867	23.07
Jul	131.82	6.3046	3.0764	0.4508	0.9022	26.79
Aug	119.71	6.8531	2.9635	0.3065	0.8449	22.45
Sep	35.32	3.698	4.8617	0.1554	0.7028	11.14
Oct	36.31	3.5563	7.1914	0.2819	0.7293	16.69
Nov	20.96	2.8765	7.4547	0.1693	0.6436	10.45
Dec	4.93	1.2159	11.8253	0.0778	0.5156	4.41

Precipitation guage location table is usually required to specify or provide the location of rain guages. It was formatted according to ArcSWAT interface for SWAT 2012, a users' guide (Winchell, Srinivasan, Di Luzio, and Arnold, 2013).

Table 3.16. Precipitation gage location table

```
ID,NAME,LAT,LONG,ELEVATION
1,p5350,0.468,35.000,1981.000
2,p5353,0.468,35.313,2178.000
3,p5356,0.468,35.625,1094.000
```

For each location, a daily precipitation data table showing precipitation on each individual day for the period of study, was prepared in ASCII format according to ArcSWAT interface for SWAT 2012, a users' guide (Winchell *et al.,* 2013).

Air Temperature and Relative Humidity Data

Table 3.17. Temperature guage location table

> A total of 8 datasets for 8 weather stations were downloaded. However, only three datasets were selected to correspond to the selected rainfall datasets. The gage location tables and daily data tables for air temperature and relative humidity were formatted according to ArcSWAT interface for SWAT 2012, a users' guide
> ID,NAME,LAT,LONG,ELEVATION
> 1,t5350,0.468,35.000,1981.000
> 2,t5353,0.468,35.313,2178.000
> 3,t5356,0.468,35.625,1094.000

Table 3.18. Relative humidity guage location table.

> ID,NAME,LAT,LONG,ELEVATION
> 1,r5350,0.468,35.000,1981.000
> 2,r5353,0.468,35.313,2178.000
> 3,r5356,0.468,35.625,1094.000

The air temperature and relative humidity datasets were used to calculate the average daily dewpoint temperature per month. The humidity values are usually expressed as percentages. However, the values in the humidity datasets were between 0 and 1. To convert them to percentage, the values were multiplied by 100. The product was used in the calculation average daily dewpoint temperature per month. Calculation of the dewpoint temperature was done using *dew02.exe* computer program (Stefan, 2003). The input file was formatted in three columns are as shown in the following sequence: maximum temperature, minimum temperature, average daily humidity.

The program gives three output items: average daily temperature in the month (tmp), average daily humidity in the month (hmd) and average daily dewpoint temperature in the month (dewpt).

Table 3.19. Average daily dewpoint temperature for station 5350 for the period 1984 – 2012.

Month	tmp max	tmp min	hmd	dewpt
Jan	28.69	13.37	44.19	9.23
Feb	30	13.82	42.73	9.57
Mar	30.19	13.7	50.95	12.39
Apr	27.28	13.46	71.63	16.03
May	25.56	12.11	78.61	16.08
Jun	23.31	12.07	81.01	15.18
Jul	22.95	12.57	79.48	14.77
Aug	24.57	12.93	77.41	15.46
Sep	27.88	12.95	64.21	14.51
Oct	27.22	13.38	65.56	14.63
Nov	26.52	13.01	62.51	13.31
Dec	27.42	12.81	52.34	10.9

Table 3.20. Average daily dewpoint temperature for station 5353 for the period 1984 – 2012.

Month	tmp max	tmp min	hmd	dewpt
Jan	26.74	10.13	49.05	8.86
Feb	27.97	10.56	46.9	9.05
Mar	27.79	11.06	54.36	11.33
Apr	25.26	11.57	72.94	14.5
May	24.28	10.02	77.75	14.47
Jun	22.68	10.54	81.2	14.34
Jul	22	11.28	81.95	14.25
Aug	23.38	11	78.91	14.43
Sep	25.61	10.07	66.37	12.81

Oct	24.94	11.32	67.94	13.13
Nov	24.46	10.96	66.73	12.44
Dec	25.52	10.14	57	10.38

Table 3.21. Average daily dewpoint temperature for station 5356 for the period 1984 – 2012.

Month	tmp max	tmp min	hmd	dewpt
Jan	28.73	10.23	48.5	10.06
Feb	29.85	10.7	46.09	10.14
Mar	29.64	11.39	52.52	12.2
Apr	27.65	12.22	66.92	14.9
May	27.09	11.51	68.21	14.64
Jun	26.42	11.62	70.32	14.75
Jul	25.67	12.12	71.44	14.65
Aug	26.85	11.87	67.5	14.41
Sep	28.44	11.09	56.65	12.51
Oct	27.54	11.81	60.51	13.15
Nov	26.67	11.19	63.17	13.13
Dec	27.58	10.3	55.54	11.44

Solar Radiation and Wind Speed Data

Solar radiation and wind speed guage location tables and daily data tables were formatted according to ArcSWAT interface for SWAT 2012, a users' guide (Winchell *et al.,* 2013).

River Discharge Data

Observed flow time series was for the time period 1st January 1984 to 31st March 2009. The data had numerous gaps as shown in the following time series plot.

Figure 3.16. Time series graph for Sosiani River flow at 1CB05 gauging station.
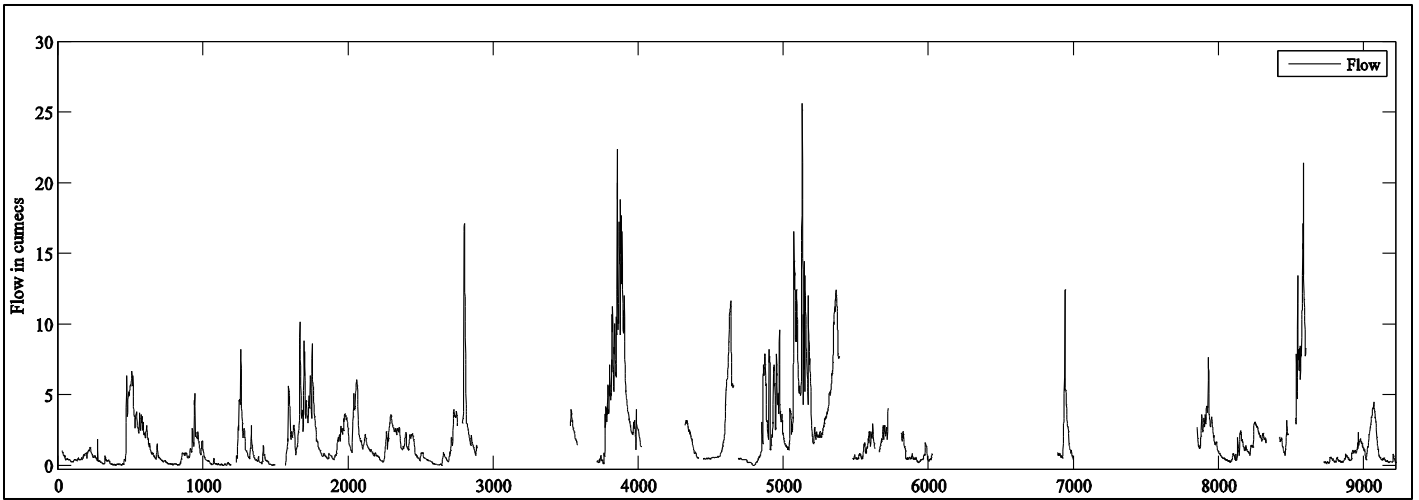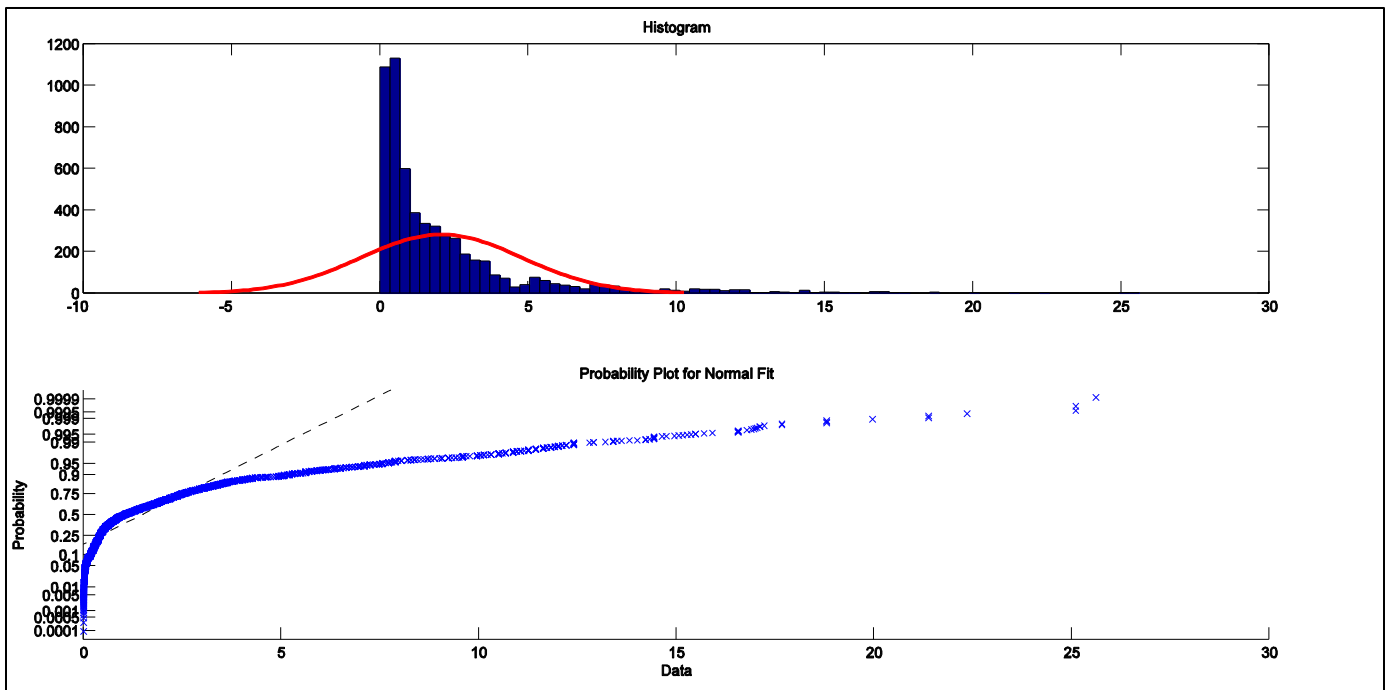

Figure 3.17. Historgram and Probability Plot for Sosiani Flow Data

The histogram is skewed to the right while the data points dissent away from the normal fit. This shows that the data does not fit a normal distribution. The skewness value for the time series is 2.8597. The skewness for a normal distribution is usually zero. The positive value shows that the data does fit a normal distribution. Kurtosis is a measure of how outlier-likely a data distribution is. Distributions that have kurtosis greater than 3 are usually more outlier-prone than

normal distribution. The kurtosis value for the dataset is 13.9642. This confirms that the dataset is more outlier-prone and dissents from a normal distribution.

3.3 Model Set-up

The process of model set up was divided into four phases. The phases comprised watershed delineation, hydrologic response unit (HRU) definition, weather data definition and writing input tables.

Watershed Delineation

A new SWAT project was created. Then the project DEM and a burn-in stream shapefile were loaded. Stream-definition was DEM-based. The minimum area to define a stream was set to 2000ha, which is 3.041 percent of the total catchment area. Outlet and inlet definition was done manually by adding the catchment outlet at GPS point 35.052, 0.632. It is from this outlet that the watershed was delineated. The process was completed by calculating sub-basin parameters.

Landuse/Soils/Slope Definition

The landuse raster dataset was loaded. The grid field on which reclassification would be based was set to VALUE. A look-up table was loaded. The landuse dataset was reclassified into SWAT landuse themes. Next, the soil raster dataset was loaded. The grid field on which reclassification would be based was set to VALUE. Under the soil database options, usersoil was checked. Then the soil look-up table was loaded. The raster soil dataset was reclassified based on the look-up table. Under slope discretization, multiple slope option was chosen. Slope classes were set to 3: 0 – 2 %, 2 – 60 % and 60 – 9999%. The process of landuse/soils/slope definition was completed by overlay of the landuse, soils and slope datasets and creation of HRU feature class.

Hydrologic Response Unit (HRU) Definition

Under HRU definition sub-interface, multiple HRUs option was chosen. The threshold was set to percentage. To llow all types of soil and classes of land use and slope in each subwatershed to be used in the simulations, threshold values were set to zero percent. The land use classes were left unrefined. Number of elevation bands was set to 2 with minimum sub-basin elevation range of 1800 metres. The process was completed by creating HRUs and writing HRU reports.

Weather Data Definition

Under the weather generator data, WGEN_CFSR_World was selected as the monthly weather database. This was followed by loading gage location tables fof rainfall, temperature, relative humidity, solar radiation and wind speed data. The tables were used to specify location of weather data stations to be used in simulation.

Writing Input Files

The write all command was used. The model returned an error during the creation of soil data tables. A new soil dataset, the digital soil map of the world (FAO-UNESCO, 1990) was used in order to resolve the error. A usersoil database created from the dataset was used to update the default SWAT usersoil database. A soil shapefile for the study area was clipped from the world soil shapefile using clipping tool in ArcMap geoprocessing. The model setup process was repeated from HRU Analysis/Landuse/Soils/Slope definition up to Write Input Tables/Database Update.

Edit SWAT Input

Under edit databases, soil parameters in the new soil database were edited to reflect the properies of the HWSD. The parameters edited include soil hydrologic group, soil albedo, soil availabe water content, soil bulk density, soil crock content, sand content, clay content, saturated hydraulic conductvity, carbon content, texture and USLE erodibility factor. The changes were made both for topsoil and sub-soil for all the soil classes in the digital soil map of the world (DSMW). The other databases were left at defualt values.

Under watershed data, only general basin data was edited. The assumption made during watershed delineation was that there were no reservoirs, point-source discharges and inlet discharges within the the catchment. Therefore, the data was not available for editing at the edit SWAT input stage. The parameters influencing rainfall-runoff were located in edit general watershed parameters section; water balance, surface runoff and reaches. The parameters included SFTMP, SMTMP, SMFMN,SMFMX, TIMP, SNOCOVMX, SNO50COV, IPET, ESCO, EPCO, EVLAI, FFCB, IEVENT, ICN, CONCOEF, SURLAG, ISED_DET.

Water balance sub-component, snowfall temperature (SFTMP), the mean air temperature at which precipitation is equally likely to be rain as snow/freezing rain, was set to zero (0). Snow

melt base temperature (SMTMP), temperature beyond which snowpack will melt, was set to zero (0). Melt factor for snow on June 21st (SMFMX) and melt factor for snow on December 21st (SMFMN) were both set to 8.0 mm of water per celsius-degree-day. This is because even this factor was not required in the area of study, melt factor for snow in the area would be high because it is in the tropics. The snow pack temperature lag factor (TIMP) was set to 1. The minimum snow water content that corresponds to 100 percent snow cover (SNOCOVMX) was set to 1. The fraction of snow volume represented by SNOCOVMX that corresponds to 50 percent snow cover (SNO50COV) was set 0.50.

Potential evapotranspiration (PET) method (IPET) was set to Penman/Monteith. Soil evaporation compensation factor (ESCO) was set at 0.95, plant uptake compensation factor was set at 1 (EPCO) while leaf area index at which no evaporation occurs from water surface (EVLAI) was set at 3. The initial water storage expressed as a fraction of field capacity water content (FFCB) was set at 0.0. Rainfall-runoff method (IEVENT) was wet daily rainfall/curve number runoff/ daily routing. The daily curve number calculation method (ICN) was set to soil moisture method. Plant ET curve number coefficient (CNCOEF) was set to 1. Surface runoff lag coefficient (SURLAG) was set to 4. Code governing calculation of daily maximum half-hour rainfall (ISED_DET) was set to use monthly half-hour rainfall value for all the days in a month.

After the edits, the SWAT files were re-written using Rewrite SWAT Input Files command. After rewrting , the model was set ready ready for simulation..

3.4 Simulation of Runoff

In the initial simulation, the following settings were made in the set-up SWAT Run phase. The period of simulation was set to begin 1st January 1984 to 31st December 2012. A daily time-step was used in the simulation. The equilibration period was set to 5 years while the rainfall distribution was set to skewed normal. After the set-up SWAT Run phase, the SWAT Run process was executed.

3.5 Simulation of Sediment Yield

Simulation of sediment yield was executed alongside runoff. The period of simulation was set to begin 1st January 1984 and end 31st December 2012. The equilibration period was set to 5 years.

3.6 Simulation of Soil Erosion

Arc-SWAT does not directly simulate soil erosion as part of its output. Therefore soil erosion was simulated using an emprical relationship between sediment yield , sediment delivery ratio and soil erosion (Ward and Trimble, 2003).

$$SDR= \left[\left(\frac{q_{peak}}{R_{peak}} \right) \left(0.78285+0.21716 \frac{Q}{R} \right) \right]^{0.56} \tag{2.16}$$

3.7 Runoff Calibration and Validation and Sensitivity Analysis

Calibration for runoff was done using SWAT-CUP parameter solution program, Parasol *(Abbaspour, 2015a)*. The method stochastiscally accounts for most sources of uncertainty and expresses the uncertainty in parameters in uniform distributions. Uncertainties in model output variables is expressed as 95% probability distributions using latin hypercube sampling. The 95% probability distribution is termed a 95PPU. Evaluation of calibration result done based on two factors: the p-factor (ranges between 0 and 100) and an R-factor (ranges between 0 and infinity).

The simulation period for the study was 1984 to 2012. The equilibration period was set to 5 years and the calibration period from 1989 to 1991. In the first iteration, 4 parameters were chosen for optimization. The parameters are groundwater delay time ,initial SCS curve number for moisture condition, baseflow alpha factor, threshold depth of water in the shallow aquifer required to return for return flow to occur, soil bulk density, available soil water contect, soil hydraulic conductivity. The number of simulations was set to 10. The sub-basin was set to the catchment level and the objective functions included Nash Sutcliffe coefficeint, p-factor, r-factor, coefficeint of determination, coffecent of determination mutliplied by coeffiecent of regression

CHAPTER FOUR

RESULTS AND DISCUSSION

4.1 Model Set-Up

Sosiani catchment has a mean elevation of 2191.32 meters, a minimum elevation of 1801 meters and a maximum elevation of 2764meters above sea level. Fifty perecent of the catchment lies above 2100 meters above sea level. The catchment was delineated into 7 sub-catchments and 113 hydrologic response units.

The main land use classes in Sosiani catchment include agricultural, mixed forest, urban commercial and rangeland (grasslands). Table 4.1 shows the areal distribution of the landuse by area in hectares and acres and by percentage of area. Figure 4.1 is a bar chart of landuse by percentage of area. Slope was classified into three classes (table 4.2). Figure 4.1 shows the distribution by percentage of area.

Table 4.1: Sosiani landuse areal distribution.

Landuse	Area [Ha]	Area [Acres]	Percent Area
Urban Commercial	3074.07	7596.18	4.67
Forest-Mixed	7231.99	17870.60	11.00
Range-Grasses	3023.93	7472.28	4.60
Agricultural Land-Generic	52430.11	129557.41	79.73

Table 4.2: Sosiani slope areal distribution

Slope Class [%]	Area [Ha]	Area [Acres]	Percent Area
0-2	7644.29	18889.42	11.62
2-60	58102.09	143573.17	88.35
60-9999	13.71	33.88	0.02

Figure 4.1: Bar chart showing distribution of landuse by area in Sosiani catchment.

Landuse and Slope Distribution by Area Percentage
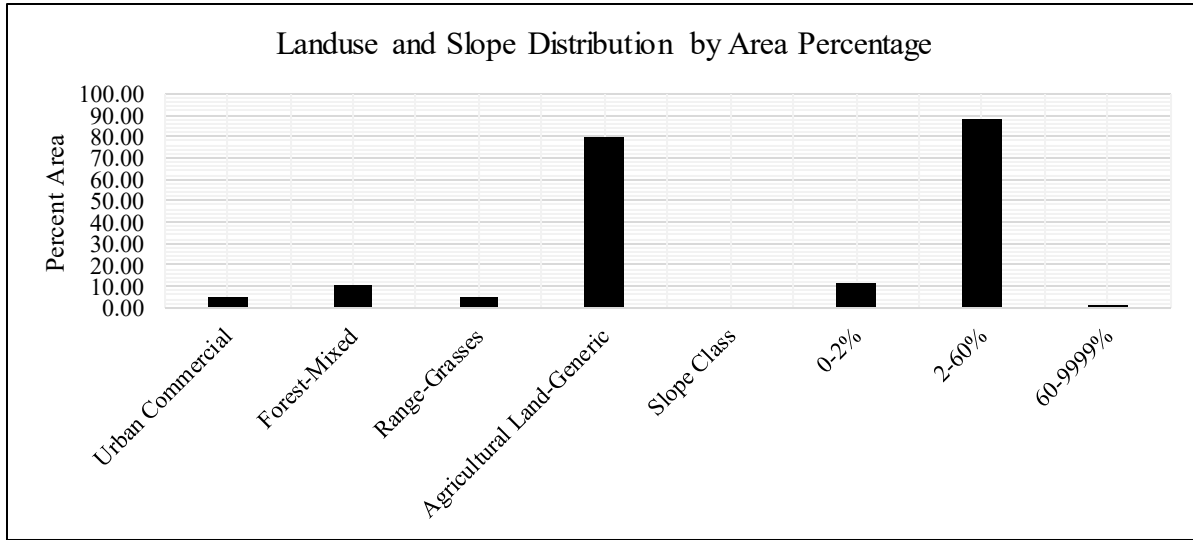
4.2 Runoff Simulation, Calibration and Validation

4.2.1 Simulation

The following graph shows a time series plot of simulated and observed mean monthly runoff before calibration of the model.

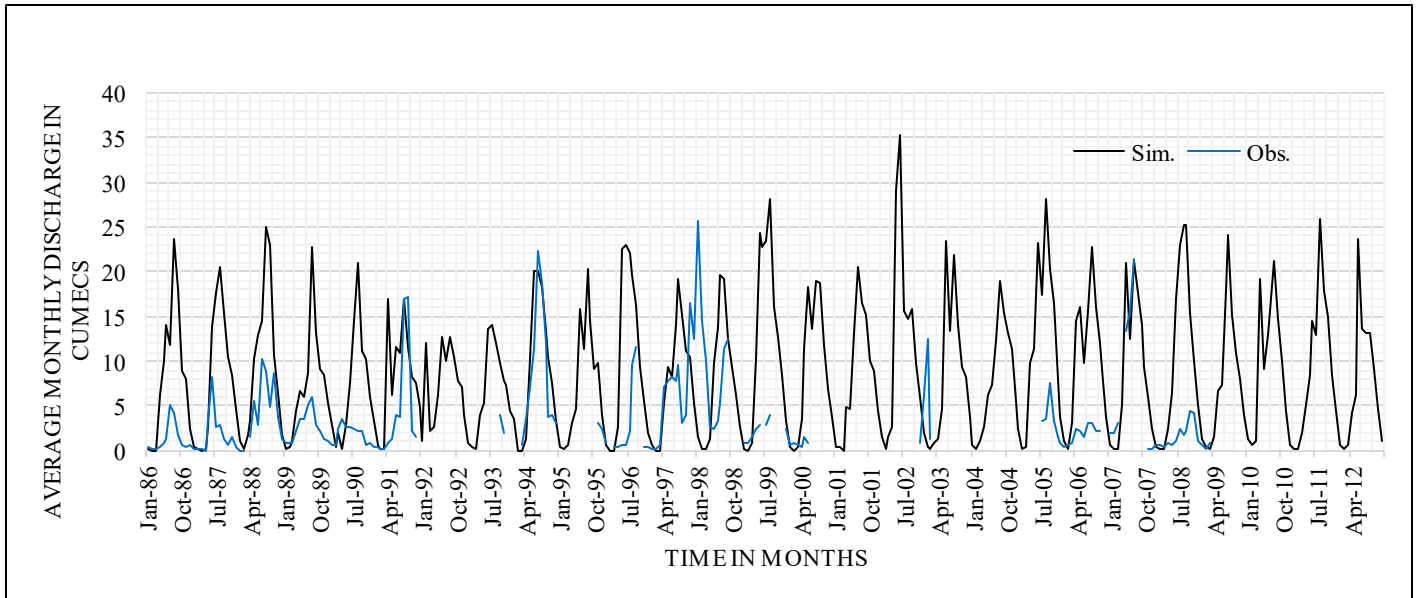Figure 4.2: Time series plot of simulated and observed mean monthly river discharge.

Figure 4.3.: Bar plot of simulated and observed long term mean monthly flow, before calibration.
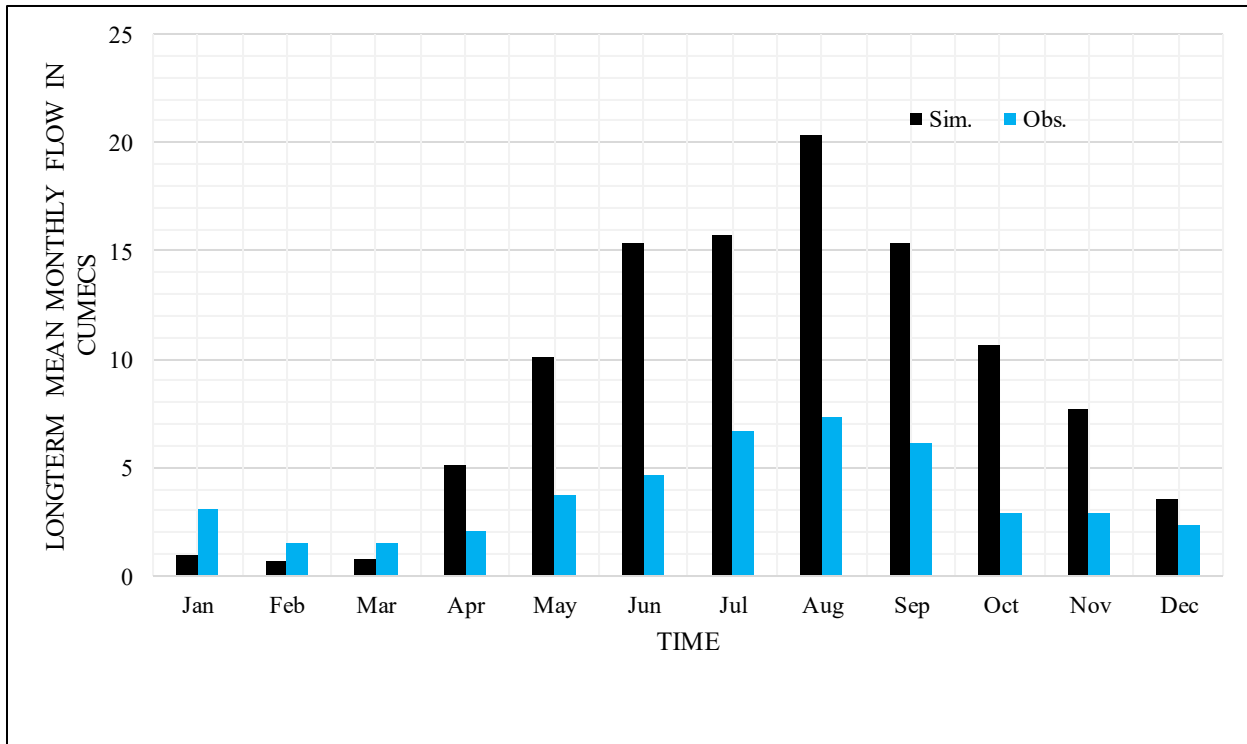

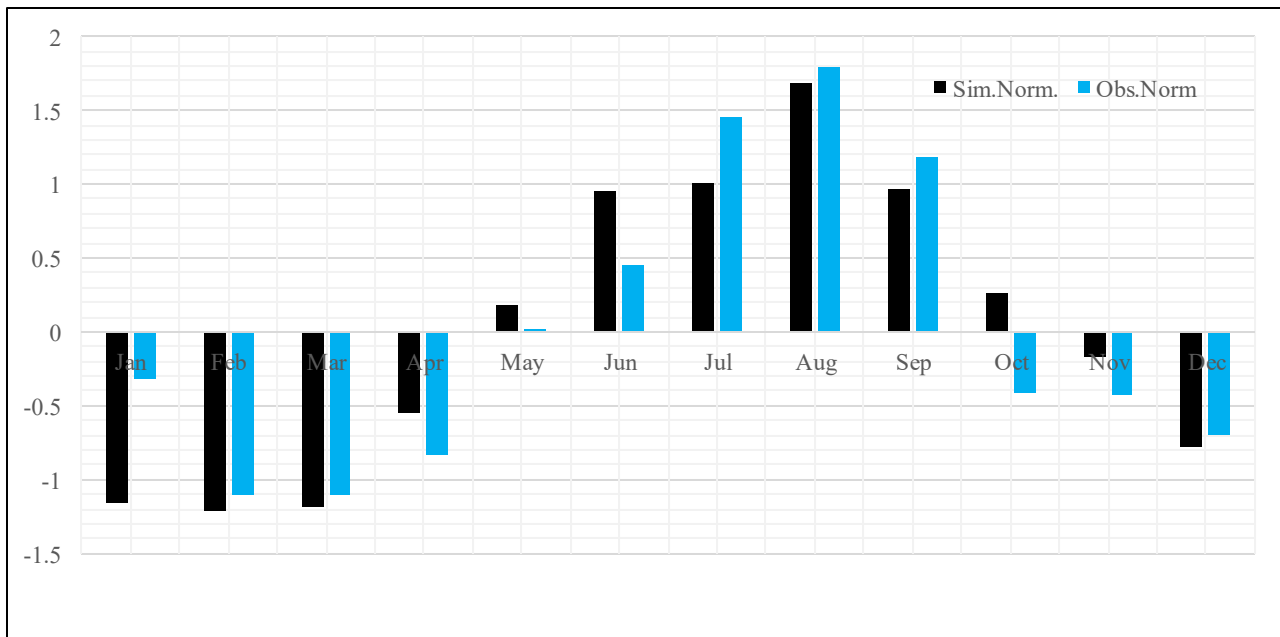Figure 4.4.: Bar plot of normalized long-term mean monthly flow.

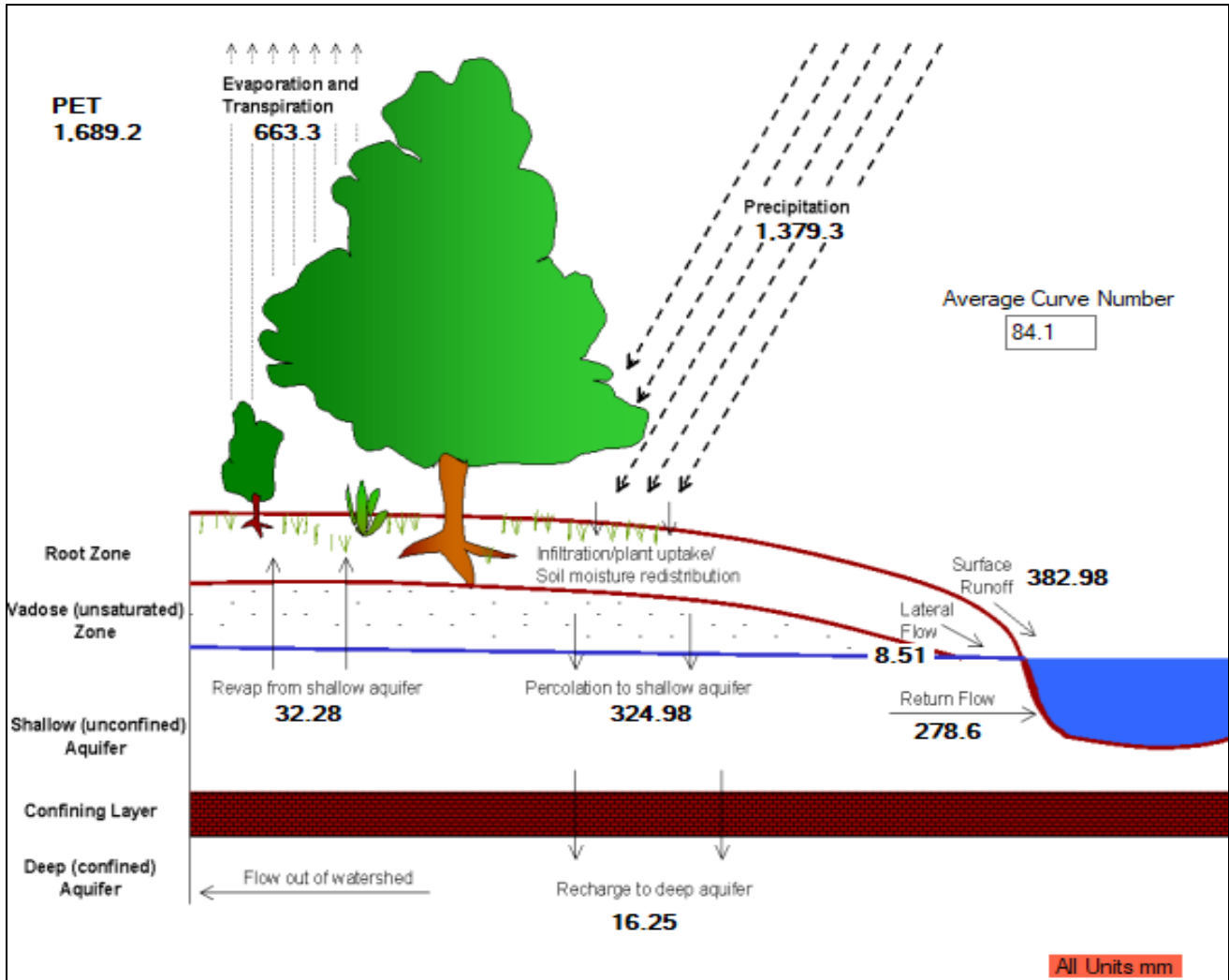Figure 4.5: Water budget before model calibration.
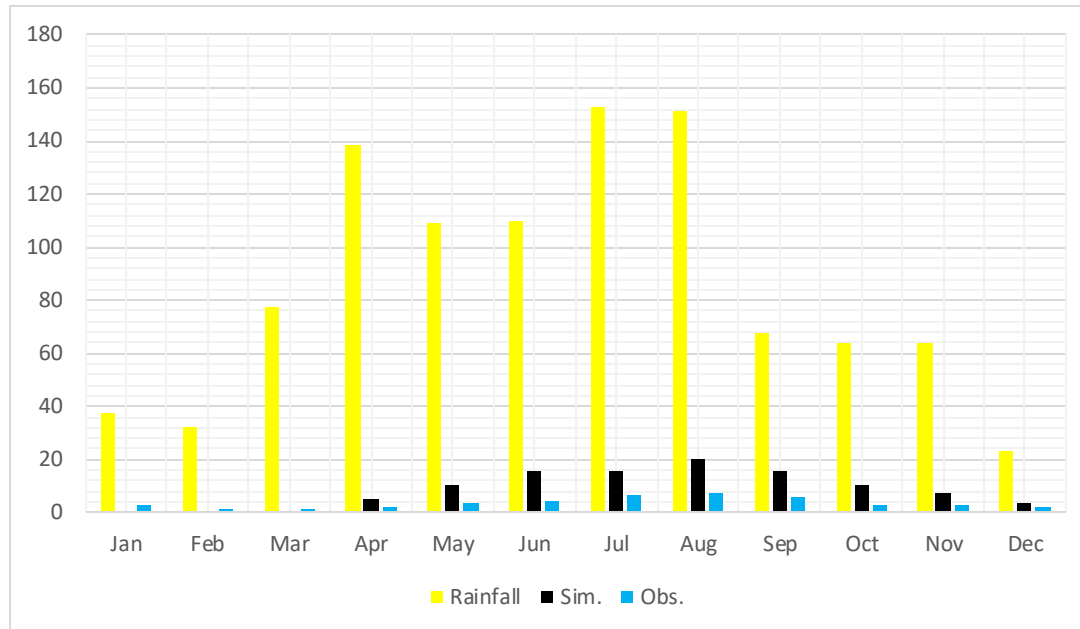
Figure 4.6: A plot of rainfall and runoff.

Table 4.3: Landuse/Land cover hydrological summary

LULC	Area [Sq.Km]	CN	AWC [mm]	USLE LS	PREC[mm]	SURQ[mm]	GWQ[mm]	ET[mm]
AGRR	523.04	85.33	161.63	1.09	1432.25	416.58	313.39	654.46
UCOM	20.87	89.42	170	0.86	1633.47	837.66	3.03	763.79
FRST	66.32	75.45	141.5	1.82	959.15	94.94	178.08	645.23
RNGE	46.16	80.12	154.57	1.55	1266.47	220.25	280.49	719.76
WATR	0.97	92	170	0.56	1513.57	0	0	1786.27
WILL	0.1	77	170	1.46	1629	247.1	494.73	831.25

4.2.2 Calibration

The following figure shows summary statistics of flow calibration results.

Figure 4.7: Summary statistics of flow calibration results.


```
Results of 5 good simulations
Variable          n       p-factor     r-factor      R2        NS        bR2        MSE
FLOW_OUT_5.txt   60       0.00         2.09          0.90     -19.92     0.3760     39.2673
```
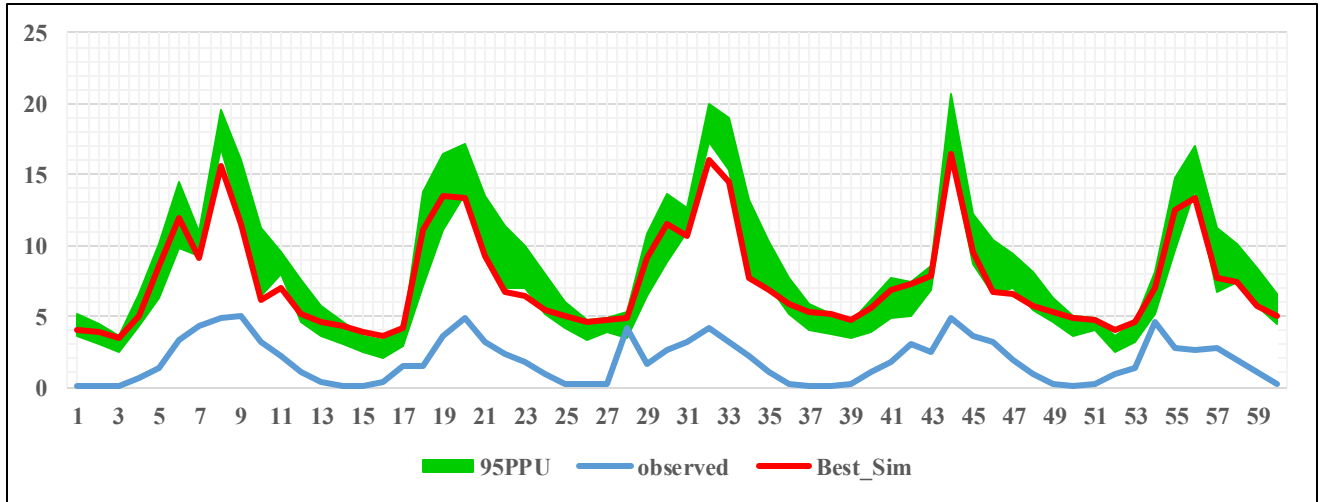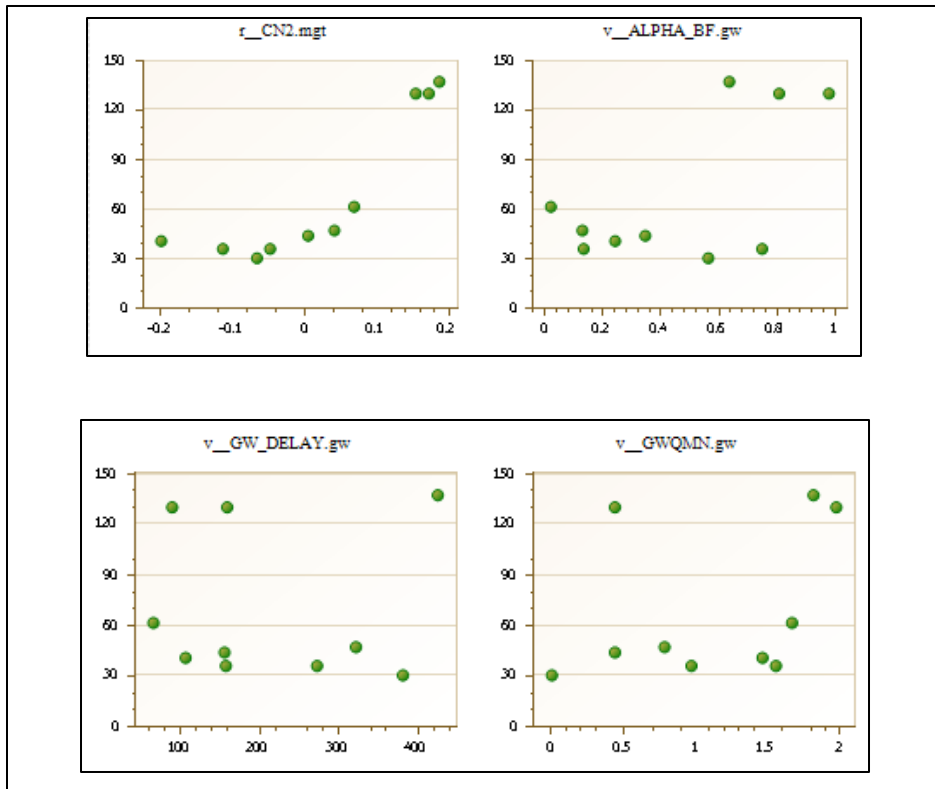
Figure 4.8: 95ppu plot for calibration results.

Figure 4.9:Dotty Plots from calibration results
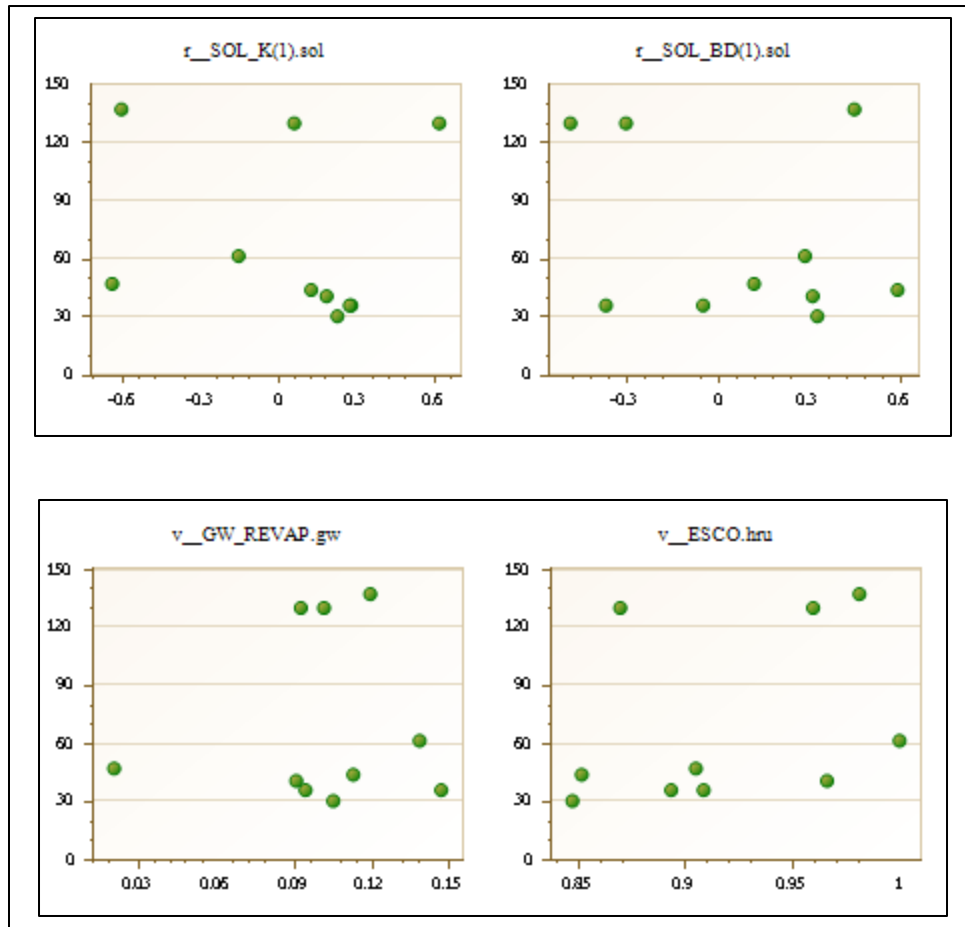
4.2.3 Validation

Figure 4.10: Summary statistic for validation

```
Results of 4 good simulations
Variable          n        p-factor     r-factor      R2         NS         bR2         MSE
FLOW_OUT_5.txt   60        0.02         1.78          0.60       -14.90     0.3468      37.7359
```

4.3 Simulation of Sediment of Yield Different Management Scenarios

4.3.1 Initial Simulation

Among other factors, sediment yield is usualy influenced by rainfall, landcover and soils. The following table shows the results of longterm mean monthly sediment yield tonnes, under default model setup scenario.

Table 4.4. Longterm mean monthly simulated sediment yield

Month	Sed. Yield [tons/ha]
Jan	49.86014815
Feb	7.292407407
Mar	48.06942593
Apr	591.0444074
May	1153.511111
June	1757.522222
July	1636.177778
Aug	2108.003704
Sept	1462.966667
Oct	900.4481481
Nov	564.3222222
Dec	201.45

4.3.2 Sediment Simulation Under Different Scenarios

Table 4.5 Sediment yield under different scenarios

Scenario	%change in Sediment Yield
Split AGRR (row crops) by 50% and add sub-landuse SPOT(sweet potatoes) by 50%	19.234%
Reduce RGNE by 20%, add sub-landuse FRST 20%	0.531%
Reduce WILL by 50% , add sub-landuse FRST 40% and SPOT 10%	2%
Combined Scenario: AGRR-39.5%; FRST-11.51%; SPOT-39.79%; RGNE-5.62%; WILL-0.0075%.	21.8%

4.4 Simulation of Soil Erosion

Peak mean monthly rainfall was estimated to 216.076mm. Annual rainfall was calculated as 1327.59mm. Peak monthly surface runoff was estimated to be 59.983mm while annual total surface runoff was estimated to be 368.539mm.

Sediment delivery ratio was calculated to be 0.4434.

Mean monthly soil erosion was estimated as shown the following table

Table 4.6: Simulated Soil Erosion.

Month	Sed. Yield [tons/ha]	Erosion [tons/ha]
Jan	49.86014815	112.4495899
Feb	7.292407407	16.4465661
Mar	48.06942593	108.4109741
Apr	591.0444074	1332.982425
May	1153.511111	2601.513557
June	1757.522222	3963.739788
July	1636.177778	3690.071669
Aug	2108.003704	4754.180659
Sept	1462.966667	3299.428658
Oct	900.4481481	2030.780668
Nov	564.3222222	1272.715882
Dec	201.45	454.3301759

4.5 Discussion

4.5.1 Data preparation and Pre-analysis

The use of Harmonized World Soil Database (HWSD) with ArcSWAT is still limited. Preparation of the dataset for use in ArcSWAT requires calculation of several parameters compared to the Digital World Soil Map. Etimation of soil hydraulic conductivity and soil

available water content using parameters form HWSD gives values that a very low compared to the values in Digital World Soil Map (DWSM).

River flow data acquired from Water Resources Authority had long periods of missing data. The available data was highly outlier prone. This consequently affected the model results as the data was not reliable. At the time of completion of the study, the researcher was unable to get observed sediment data. Consequently, the model was not calibrated for sediment yield.

4.5.2 Model Set-up

The catchment was delineated into 9 sub-catchments, three slope classes and 166 HRUs. Sosiani catchment landuse/landcover is distributed in the as follows: 79% Agriculture row crops, 10% forest, 7% grassland, 0.015% willow, 0.148 % water and 3.166% urban commercial. This indicated that most runoff and sediment yield in the catchment would be generated from agricultural land. Sosiani soils are distributed as 64% orthic ferralsols, 23% humic nitisols, 12% lithosols and 1% eutric nitisols.

4.5.3 Runoff Simulation, Calibration, Validation and Sensitivity Aanlysis

The model ove-estimated both high flows and low flows during simulation, calibration and validation. This behaviour can be attributed to the type of rainfall datasets used, and the quality of observed flow data.

4.5.4 Simulation of Sediment Yield and Soil Erosion

The researcher was unable obtain observed sediment data for model calibration. Consequently, the model was not calibrated for sediment. However, simulation results were excessive for a tropical catchment. The excessive sediment yield simulation results can be explained by model simulation of runoff. The runoff simulation output directly affected the output of sediment yield simulation. Erosion simulation output was also overstimated because erosion was estimated from an empricial equation whose main inputs were runoff, sediment yield and rainfall.

4.5.5 Scenarios for Management

The study established that agricuture contributed the largest percentage of sediment yield from Sosiani catchment. Very high sediment yield was also simulated from humic nitisols which account for 23% of soils in Sosiani catchment. Low sediment yield was observed from forest. Scenario testing revealed that a combination 39.5% agricultural row crops;11.51% forest; 39.79% cover crops ; 5.62% grasslands and 0.0075% shrubs can reduce catchment sediment yield by 22%.

CHAPTER FIVE

CONCLUSION AND RECOMMENDATIONS

5.1. Conclusion

The study concludes that: firstly, increase in rainfall magnitude increases runoff. Months that had less rainfall had low magnitudes of runoff. Secondly, increase in rainfall magnitude increases sediment yield while decrease in rainfall decreases sediment yield, factors remaining constant. This is because rainfall and runoff both have an effect on erosion and sediment yield. However, increase in closed land cover such as planting sweet potoatoes will reduce soil erosion and sediment yield even with increasing rainfall magnitude. Thirdly, soil type, landuse, rainfall-runoff are major drivers of soil erosion and sediment yield in Sosiani catchment. For instance, the HRUs that had agricultural row crops and humic nitisol soils produced the highest magnitudes of sediment. To abate erosion in highly erodible soils, increase in vegetative landcover can be an immediate action.

The study concludes that simulated results were not satisfactory because of the datasets used. The quality of input datasets directly affected the ouput of the model. We conclude too that without reliable observed variable datasets, was difficult to establish whether the model correctly simulated the local hydrologic conditions. We conclude that even though the magnitude model results was much higher than the magnitude of corresponding observed, a plot of residuals of simulated and observed followed the same pattern, indicating that the model can be used to simulate correctly simulate the behaviour of the catchment once the integrity of the input datasets is assured.

5.2 Recommendations

The study recommends that another attempt to model Sosiani catchment using ArcSWAT may require to thoroughly interrogate rainfall datasets used. It may be necessary too to acertain the integrity of the observed river flow before using the datasets for model calibration. The river flow dataset was higly outlier-prone. It may be necessary the reason for this behaviour.

Lastly, the study recommends that erosion control on agricultural lands through agroforestry and planting of cover crops that than open row crops can to a large extent reduce soil erosion and sediment yield in Sosiani catchment.

REFERENCES

Abbaspour, K. C. (2015a). SWAT-CUP: SWAT Calibration and Uncertainty Programs-A User Manual. Eawag: Swiss Federal Institute of Aquatic Science and Technology.

Abbaspour, K. C. (2015b). SWAT-CUP: SWAT Calibration and Uncertainty Programs-A User Manual. Eawag: Swiss Federal Institute of Aquatic Science and Technology.

Abrams, M. (1999). The Advanced Space borne Thermal Emission and Reflection Radiometer (ASTER): data products for the high spatial resolution imager on NASA's EOS-AM1 platform. *International Journal of Remote Sensing*, *00*(00), 1–12.

Adeogun, A. G., Sule, B. F., and Salami, A. W. (2016). Cost effectiveness of sediment management strategies for mitigation of sedimentation at Jebba Hydropower reservoir, Nigeria. *Journal of King Saud University - Engineering Sciences*.

Arabi, M., Frankenberger, J. R., Engel, B. A., and Arnold, J. G. (2008). Representation of agricultural conservation practices with SWAT. *Hydrological Processes*, *22*(16), 3042–3055.

Arnold, J. G., Kiniry, J. R., Srinivasan, R., Williams, J. R., Haney, E. B., and Neitsch, S. (2011). Soil and Water Assessment Tool Input-Output File Documentation Version 2009. Soil and Water Research Laboratory-Agricultural Research Service Blackland Research Center-Texas Agrilife Research.

Arnold, J. G., Moriasi, D. N., Gassman, P. W., Abbaspour, K. C., White, M. J., Srinivasan, R., … Jha, M. K. (2012). SWAT: model use, calibration, and validation. *Transactions of American Society Agricultural and Biological Engineers*, *55*(4), 1491–1508.

Aura, M., Christopher, Raburu, O., Phillip, and Herrmann, J. (2011). Macroinvertebrates' community structure in Rivers Kipkaren and Sosiani, River Nzoia basin, Kenya. *Journal of Ecology and the Natural Environment*, *3*(2), 39–46.

Bagnold, R. A. (1977a). Bed load transport by natural rivers. *Water Resources Research*, *13*(2), 303–312.

Bagnold, R. A. (1977b). Bed load transport by natural rivers. *Water Resources Research*, *13*(2), 303–312.

Barasa, B., Namulunda. (2014). *Assessing Impacts of Landuse Changes on Flood Occurrence in Sosiani River Basin in Kenya.* (Master Thesis). International Centre for Water and Hazard Risk Management under the auspices of UNESCO, Japan.

Ben Salah, N. C., and Abida, H. (2016a). Runoff and sediment yield modeling using SWAT model: case of Wadi Hatab basin, central Tunisia. *Arabian Journal of Geosciences*, *9*(11).

Ben Salah, N. C., and Abida, H. (2016b). Runoff and sediment yield modeling using SWAT model: case of Wadi Hatab basin, central Tunisia. *Arabian Journal of Geosciences*, *9*(11).

Bingner, R. L., Theurer, F. D., and Yuan, Y. (2015). AnnAGNPS Technical Processes Documentation. Version 5.4. USDA–ARC National Sedimentation Lab. and USDA–NRCS National. Water and Climate Center.

Bisantino, T., Bingner, R., Chouaib, W., Gentile, F., and Trisorio Liuzzi, G. (2015). Estimation of Runoff, Peak Discharge and Sediment Load at the Event Scale in a Medium-Size Mediterranean Watershed Using the AnnAGNPS Model: AnnAGNPS EVALUATION FOR RUNOFF, PEAK DISCHARGE AND SEDIMENT LOAD. *Land Degradation and Development*, *26*(4), 340–355.

Blanco-Canqui, H., and Lal, R. (2010). *Principles of Soil Conservation and Management.* Dordrecht: Springer Netherlands.

Borah, D. K., Krug, E. C., and Yoder, D. (2008). Watershed Sediment Yield. In M. Garcia (Ed.), *Sedimentation Engineering* (pp. 827–858). Reston, VA: American Society of Civil Engineers.

Chaubey, I., Cotter, A. S., Costello, T. A., and Soerens, T. S. (2005). Effect of DEM data resolution on SWAT output uncertainty. *Hydrological Processes*, *19*(3), 621–628.

Chen, W.-F., and Liew, J. Y. R. (Eds.). (2003a). *The civil engineering handbook*. Boca Raton [FL]: CRC Press.

Cuomo, S., Della Sala, M., and Novità, A. (2015). Physically based modelling of soil erosion induced by rainfall in small mountain basins. *Geomorphology*, *243*, 106–115.

Defersha, M. B., Melesse, A. M., and McClain, M. E. (2012). Watershed scale application of WEPP and EROSION 3D models for assessment of potential sediment source areas and runoff flux in the Mara River Basin, Kenya. *CATENA*, *95*, 63–72.

Exelis. (2013). Environment for Visualizing Images (ENVI) version 5.1. Harris Corporation.

Fang, N.-F., Shi, Z.-H., Li, L., Guo, Z.-L., Liu, Q.-J., and Ai, L. (2012). The effects of rainfall regimes and land use changes on runoff and soil loss in a small mountainous watershed. *CATENA*, *99*, 1–8.

FAO. (2015). *Status of the world's soil resources: main report.* Rome: FAO: ITPS. FAO. (2016). *Mainstreaming Ecosystem Services and Biodiversity into Agricultural Production and Management in East Africa.* Rome: FAO: ITPS.

FAO/IIASA/ISRIC/ISS-CAS/JRC. (2009). *Harmonized World Soil Database (Version 1.2).* Rome, Italy and IIASA, Laxenburg, Austria: FAO.

FAO-UNESCO. (1990). *Digital World Soil Map*. FAO.

Farr, T. G., Rosen, P. A., Caro, E., Crippen, R., Duren, R., Hensley, S., … Alsdorf, D. (2007). The Shuttle Radar Topography Mission. *Reviews of Geophysics*, *45*(2).

Feng, C. J. (1995). *Soil Conservation Handbook*. Republic of China: Food and Fertilizer Technology Center for the Asian and Pacific Region.

Forkuor, G., and Maathuis, B. (2012). Comparison of SRTM and ASTER derived digital elevation models over two Regions in Ghana – Implications for hydrological and environmental modeling. In *Studies on Environmental and Applied Geomorphology*. INTECH Open Access Publisher.

Foster, G. R., Meyer, L. D., and Onstad, C. A. (1977). An erosion equation derived from basic erosion principles. *Transactions of American Society Agricultural and Biological Engineers*, *20*(4), 678–682.

Gassman, P. W., Reyes, M. R., Green, C. H., and Arnold, J. G. (2007). The Soil and Water Assessment Tool: historical developments, applications and future research directions. *Transactions of American Society Agricultural and Biological Engineers*, *50*(4), 1211–1250.

Geza, M., and McCray, J. E. (2008). Effects of soil data resolution on SWAT model stream flow and water quality predictions. *Journal of Environmental Management*, *88*(3), 393–406.

Gijsman, A., Thornton, P., and Hoogenboom, G. (2007). Using the WISE Database to Parameterize Soil Inputs for Crop Simulation Models. *Computers and Electronics in Agriculture*, *56*(2), 85–100.

GoK. (2013). National Land Reclamation Policy. Government Printer. Nairobi.

Green, W. H., and Ampt, G. A. (1911). Studies on Soil Physics 1. The Flow of Air and Water through Soils. *Journal of Agricultural Sciences*, *4*, 11–24.

Gupta, H. V., Beven, K. J., and Wagener, T. (2005). Model Calibration and Uncertainty Estimation. In M. G. Anderson and J. J. McDonnell (Eds.), *Encyclopedia of Hydrological Sciences*. Chichester, UK: John Wiley and Sons, Ltd.

Hargreaves, G. L., Hargreaves, G. H., and Riley, J. P. (1985). Agricultural Benefits for Senegal River Basin. *Journal of Irrigation and Drainage*, *111*(2), 113–124.

Hillston, J. (2003, September 19). Model Validation and Verification. University of Edinburgh.

Hunink, J. E., Niadas, I. A., Antonaropoulos, P., Droogers, P., and de Vente, J. (2013a). Targeting of intervention areas to reduce reservoir sedimentation in the Tana catchment (Kenya) using SWAT. *Hydrological Sciences Journal*, *58*(3), 600–614.

Hunink, J. E., Niadas, I. A., Antonaropoulos, P., Droogers, P., and de Vente, J. (2013b). Targeting of intervention areas to reduce reservoir sedimentation in the Tana catchment (Kenya) using SWAT. *Hydrological Sciences Journal*, *58*(3), 600–614.

Jha, M., Gassman, P.W., Secchi, S., Gu, R., and Arnold, J. (2004). Effect of Watershed Subdivision on SWAT Flow, Sediment, and Nutrient Predictions. *Journal of American Water Resources Association*, *40*(3), 811–825.

Kasangaki, A., Chapman, L. J., and Balirwa, J. (2008). Land use and the ecology of benthic macroinvertebrate assemblages of high-altitude rainforest streams in Uganda. *Freshwater Biology*, *53*(4), 681–697.

Kosmas, C., Danalatos, N., Cammeraat, L. H., Chabart, M., Diamantopoulos, J., Farand, R., … Vacca, A. (1997). The effect of land use on runoff and soil erosion rates under Mediterranean conditions. *CATENA*, *29*(1), 45–59

Laflen, J. M., Lane, L. J., and Foster, G. R. (1991). WEPP: A new generation of erosion prediction technology. *Journal of Soil and Water Conservation*, *46*(1), 34–38.

Langbein, W. B., and Schumm, S. A. (1958). Yield of sediment in relation to mean annual precipitation. *Transactions, American Geophysical Union*, *39*(6), 1076.

Licciardello, F., Zema, D. A., Zimbone, S. M., and Bingner, R. L. (2007). Runoff and soil erosion evaluation by the ANNAGNPS model in a small Mediterranean watershed. *Transactions of American Society Agricultural and Biological Engineers*, *50*(5), 1585–1593.

Loucks, D. P., Beek, E. van, and Stedinger, J. R. (2005). *Water resources systems planning and management: an introduction to methods, models and applications*. Paris: UNESCO.

Lowell, K., and Jaton, A. (Eds.). (1999). *Spatial accuracy assessment: land information uncertainty in natural resources*. Chelsea, Mich: Ann Arbor Press.

Maloba, J., Joab, Khaemba, A., Njenga, M., and Akali, N., Moses. (2016). Effects of increased land use changes on run off and sediment yield in the upper Nzoia catchment. *International Journal of Civil Engineering and Technology*, *7*(2), 76–94.

Manning, R. (1891). On the Flow of Water in Open Channels and Pipes. *Transactions of the Institution of Civil Engineers of Ireland*, *20*, 161–207.

Minella, J. P. G., Merten, G. H., Reichert, J. M., and Clarke, R. T. (2008). Estimating suspended sediment concentrations from turbidity measurements and the calibration problem. *Hydrological Processes*, *22*(12), 1819–1830.

MINITAB Inc. (2004). MINITAB Statistical Software (Version 14.12.0). MINITAB Inc.

Mishra, S. K., and Singh, V. P. (2003). *Soil Conservation Service Curve Number (SCS-CN) Methodology* (Vol. 42). Dordrecht: Springer Netherlands.

Monteith, J. L. (1965). Evaporation and the Environment. In *The State and Movement of Water in Living Things* (pp. 205–234). London, U.K.: Cambridge University Press.

Morgan, R. P. C. (2005). *Soil erosion and conservation* (3rd ed). Malden, MA: Blackwell Pub.

Morgan, R. P. C., and Nearing, M. A. (Eds.). (2011). *Handbook of erosion modelling*. Chichester, West Sussex, UK; Hoboken, NJ: Wiley-Blackwell.

Moriasi, D. N., and Starks, P. J. (2010). Effects of the resolution of soil dataset and precipitation dataset on SWAT2005 streamflow calibration parameters and simulation accuracy. *Journal of Soil and Water Conservation*, *65*(2), 63–78.

Mulinge, W., Gicheru, P., Murithi, F., Maingi, P., Kihiu, E., and Kirui, O., K. (2015). Economics of Land Degradation in Kenya. *ZEF- Policy Brief No.16, Zentrum Für Entwicklungsforschung, Bonn*.

Mutua, B. M., Klik, A., and Loiskandl, W. (2006). Modelling soil erosion and sediment yield at a catchment scale: the case of Masinga catchment, Kenya. *Land Degradation and Development*, *17*(5), 557–570.

Mwangi, J. K., Shisanya, C. A., Gathenya, J. M., Namirembe, S., and Moriasi, D. N. (2015a). A modeling approach to evaluate the impact of conservation practices on water and sediment yield in Sasumua Watershed, Kenya. *Journal of Soil and Water Conservation*, *70*(2), 75–90.

Mwangi, J. K., Shisanya, C. A., Gathenya, J. M., Namirembe, S., and Moriasi, D. N. (2015b). A modeling approach to evaluate the impact of conservation practices on water and sediment yield in Sasumua Watershed, Kenya. *Journal of Soil and Water Conservation*, *70*(2), 75–90.

Nash, J. E., and Sutcliffe, J. V. (1970). River flow forecasting through conceptual models part I — A discussion of principles. *Journal of Hydrology*, *10*(3), 282–290.

Natural Resources Conservation Service. (1983). Part 630. Section 4, Hydrology, Chapter 19, Transmission Losses. In *National Engineering Handbook*. USA: United States Department of Agriculture.

Natural Resources Conservation Service. (2007). Part 630 Hydrology, Chapter 7, Hydrologic Soil Groups. In *National Engineering Handbook*. USA: United States Department of Agriculture.

NCEP. (2017). Global Weather Data for SWAT. Retrieved 15 May 2017, from http://swat.tamu.edu/media/115170/swat-weatherdatabase.7z

Nearing, M. A., Jetten, V., Baffaut, C., Cerdan, O., Couturier, A., Hernandez, M., … van Oost, K. (2005). Modeling response of soil erosion and runoff to changes in precipitation and cover. *CATENA*, *61*(2–3), 131–154.

Neitsch, S.., Arnold, J. G., Kiniry, J. R., and Williams Grassland, J. R. (2011, September). Soil and Water Assessment Tool Theoretical Documentation Version 2009. Soil and Water Research Laboratory-Agricultural Research Service Blackland Research Center-Texas Agrilife Research.

NSF OpenTopography Facility. (2013). Shuttle Radar Topography Mission (SRTM) 90m. NSF OpenTopography Facility.

Obalum, S. E., Buri, M. M., Nwite, J. C., Hermansah, Watanabe, Y., Igwe, C. A., and Wakatsuki, T. (2012). Soil Degradation-Induced Decline in Productivity of Sub-Saharan African Soils: The Prospects of Looking Downwards the Lowlands with the *Sawah* Eco technology. *Applied and Environmental Soil Science*, *2012*, 1–10.

Ontumbi, G., Obando, J., and Ondieki, C. (2015). The Influence of Agricultural Activities on the Water Quality of the River Sosiani in Uasin Gishu County, Kenya. *International Journal of Research in Agricultural Sciences*, *2*(1), 2348 – 3997.

Oruta, J., Nyakora. (2016). Is Sosiani River Healthy? Investigating the Relationship between Water Quality Indicators and the Macroinvertebrate Assemblages in Sosiani River. *International Journal of Geography and Geology*, *5*(12), 259–280.

Osman, K. T. (2014). *Soil Degradation, Conservation and Remediation*. Dordrecht: Springer Netherlands.

Owens, P. N., and Collins, A. J. (Eds.). (2006). *Soil erosion and sediment redistribution in river catchments: measurement, modelling, and management*. Wallingford, UK; Cambridge, MA: CABI Pub.

Pandey, A., Chowdary, V. M., Mal, B. C., and Billib, M. (2008). Runoff and sediment yield modeling from a small agricultural watershed in India using the WEPP model. *Journal of Hydrology*, *348*(3–4), 305–319.

Pandey, A., Himanshu, S. K., Mishra, S. K., and Singh, V. P. (2016a). Physically based soil erosion and sediment yield models revisited. *CATENA*, *147*, 595–620.

Pandey, A., Himanshu, S. K., Mishra, S. K., and Singh, V. P. (2016b). Physically based soil erosion and sediment yield models revisited. *CATENA*, *147*, 595–620.

Pimentel, D. eds. (1993). *World Soil Conservation and Erosion* (First). New York, USA: Cambridge University Press.

Post, D. A., and Jakeman, A. J. (1996). Relationships Between Catchment Attributes and Hydrological Response Characteristics in Small Australian Mountain Ash Catchments. *Hydrological Processes*, *10*(6), 877–892.

Priestley, C. H. B., and Taylor, R. J. (1972). On the Assessment of Surface Heat Flux and Evaporation using Large-Scale Parameters. *Monthly Weather Review*, *100*, 81–92.

QGIS Development Team. (2017). Quantum Geographic Information System. QGIS.Org.

Raclot, D., and Albergel, J. (2006). Runoff and water erosion modelling using WEPP on a Mediterranean cultivated catchment. *Physics and Chemistry of the Earth, Parts A/B/C*, *31*(17), 1038–1047.

Renard, K. G., Foster, G. R., Weesies, G. A., and Porter, J. P. (1991). RUSLE: revised universal soil loss equation. *Journal of Soil Water Conservation*, *46*(1), 30–33.

Rhode Island State Conservation Committee. (2014). *Rhode Island Soil Erosion and Sediment Control Handbook*. Providence, Rhode Island 02908: Rhode Island Department of Environmental Management.

Rodríguez-Blanco, M. L., Arias, R., Taboada-Castro, M. M., Nunes, J. P., Keizer, J. J., and Taboada-Castro, M. T. (2016). Sediment Yield at Catchment Scale Using the SWAT (Soil and Water Assessment Tool) Model: *Soil Science*, *181*(7), 326–334.

Saxton, K. E. (2007). SPAW model (Version 6.02.75). USDA-ARS.

Saxton, K. E., and Rawls, W. J. (2006). Soil Water Characteristic Estimates by Texture and Organic Matter for Hydrologic Solutions. *Soil Science Society of America Journal*, *70*(5), 1569.

Schumann, A. H. (1998). Thiessen Polygon. In *Encyclopedia of Hydrology and Lakes* (pp. 648–649). Dordrecht: Springer Netherlands.

Shrestha, S., Babel, M. S., Das Gupta, A., and Kazama, F. (2006). Evaluation of annualized agricultural nonpoint source model for a watershed in the Siwalik Hills of Nepal. *Environmental Modelling and Software*, *21*(7), 961–975.

Stefan, (Liersch. (2003). *dew02.exe* [MS DOS]. Berlin.

Swamee, P. K., and Chahar, B. R. (2015). *Design of Canals*. New Delhi: Springer India.

Umit, D. (2015). Modeling Sediment Yield and Deposition Using the Swat Model: A Case Study of Cubuk I and Cubuk Ii Reservoirs, Turkey (PhD Thesis). Colorado State University, Fort Collins, Colorado.

USGS. (2017). Earth Explorer. Retrieved 14 May 2017, from https://earthexplorer.usgs.gov/

Wantzen, K., and Mol, J. (2013). Soil Erosion from Agriculture and Mining: A Threat to Tropical Stream Ecosystems. *Agriculture*, *3*(4), 660–683.

Ward, A. D., and Trimble, S. W. (2003). *Environmental Hydrology, Second Edition*. Hoboken: CRC Press.

Wass, P. D., and Leeks, G. J. L. (1999). Suspended sediment fluxes in the Humber catchment, UK. *Hydrological Processes*, *13*(7), 935–953.

Waswa, B., Shaban. (2012, September). *Assessment of Land Degradation Patterns in Western Kenya: Implications for Restoration and Rehabilitation* (PhD Thesis). Zentrum für Entwicklungsforschung, University of Bonn, Germany.

White, M. J., Harmel, R. D., Arnold, J. G., and Williams, J. R. (2014). SWAT Check: A Screening Tool to Assist Users in the Identification of Potential Model Application Problems. *Journal of Environment Quality*, *43*(1), 208.

Williams, J. R. (1969). Flood Routing with Variable Travel Time or Variable Storage Coefficients. *Transactions of American Society Agricultural and Biological Engineers*, *12*(1), 100–103.

Williams, J. R., and Berndt, H. (1977). Sediment yield prediction based on watershed hydrology. *Transactions of the American Society of Agricultural and Biological Engineers*, *20*(6), 1100–1104.

Wilson, E. M. (1969). *Engineering Hydrology*. London: Macmillan Education UK.

Winchell, M., Srinivasan, R., Di Luzio, M., and Arnold, J. (2013). ArcSWAT Interface for SWAT 2012: A user's guide. Soil and Water Research Laboratory-Agricultural Research Service Blackland Research Center-Texas Agrilife Research.

WWF. (2016, December 22). Soil erosion and degradation. Retrieved 22 December 2016, from http://www.worldwildlife.org/threats/soil-erosion-and-degradation

Yuan, Y., Locke, M. A., and Bingner, R. L. (2008). Annualized Agricultural Non-Point Source model application for Mississippi Delta Beasley Lake watershed conservation practices assessment. *Journal of Soil and Water Conservation*, *63*(6), 542–551.